

Classification of three-dimensional nonlinear sloshing in a square-base tank with finite depth

O.M. Faltinsen^{a,*}, O.F. Rognebakke^b, A.N. Timokha^c

^a*Department of Marine Technology, NTNU, N-7491 Trondheim, Norway*

^b*Centre for Ships and Ocean Structures, NTNU, N-7491 Trondheim, Norway*

^c*Friedrich-Schiller-Universität Jena, Ernst-Abbe-Platz 2-4, Jena, 07745, Germany*

Received 27 November 2003; accepted 18 August 2004

Available online 2 January 2005

Abstract

The paper classifies steady state three-dimensional resonant waves in a square-base tank by using the asymptotic modal system proposed by the authors in 2003. The effective frequency domains of stable steady state motions are analysed versus mean fluid depths and forcing amplitude. The results are validated by experiments both qualitatively and quantitatively. © 2004 Elsevier Ltd. All rights reserved.

1. Introduction

Three-dimensional fluid sloshing in smooth tanks is of concern in various engineering applications. One particularly challenging example is prismatic membrane tanks for transportation of liquefied natural gas (LNG). Since the length and breadth of such tanks are often similar in size, three-dimensional flow phenomena may be significant. Even if a tank oscillates with a small amplitude, forcing frequencies in the vicinity of a natural frequency for the fluid motion inside a smooth tank lead to violent surface wave response. Experimental investigations of realistic ship motions and tank dimensions shows that combined sway/surge/roll/pitch forcing (see Fig. 1) near the lowest natural frequency causes the violent sloshing and potentially dangerous loads on the ship tanks (Abramson, 1966; Abramson et al., 1974). This paper classifies the full set of three-dimensional resonant steady state waves occurring due to two types of harmonic forcing (longitudinal and diagonal) in a square-base tank. The analysis is based on the analytically oriented modal approach by Faltinsen et al. (2003). Qualitative conclusions are accompanied by direct numerical simulations (by using the modal system) as well as experimental validation. Since total hydrodynamic loads on the ship tank due to sloshing are of concern in predictions of ship motions and for dimensioning possible supports of the tank structure, the paper treats the evaluation of horizontal hydrodynamic forces due to sloshing.

Sloshing in smooth tanks with finite (non-small) mean depth can be described in the framework of a potential irrotational flow model of an incompressible fluid. This point has been documented by comparison of theoretical and experimental results by Abramson (1966), Mikishev (1978) and recently, in the framework of the modal methods for two-dimensional flows by Faltinsen et al. (2000) and Faltinsen and Timokha (2001) for the depth/breadth ratio $h > 0.27$. A requirement is also the absence of strong local phenomena like extensive free-surface run-up and overturning near the wall, wave breaking in the middle of the free surface and roof impact, which may dramatically increase dissipative effects (Yalla, 2001; Rognebakke and Faltinsen, 2000). Current achievements of the potential fluid sloshing theory

*Corresponding author. Tel.: +47 73 59 55 26.

E-mail address: oddfal@marin.ntnu.no (O.M. Faltinsen).

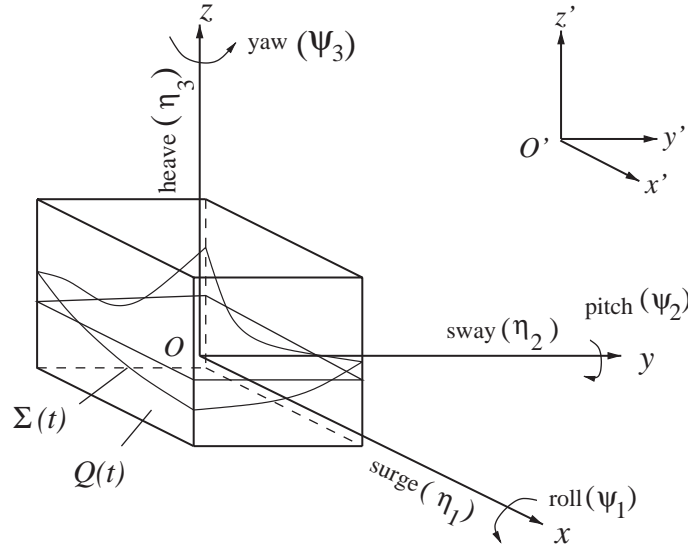


Fig. 1. Fluid sloshing in a moving tank. The rigid tank rotational velocity $\omega = (\omega_1, \omega_2, \omega_3) = \frac{d}{dt}(\psi_1, \psi_2, \psi_3)$ and translatory velocity $\mathbf{v}_O = (v_{O1}, v_{O2}, v_{O3}) = \frac{d}{dt}(\eta_1, \eta_2, \eta_3)$ are considered in the moving body-fixed coordinate system $Oxyz$ framed with the rigid tank. The $O'x'y'z'$ -system is earth-fixed.

related to this study are reviewed by Ibrahim et al. (2001) and Faltinsen and Timokha (2002b). Three different approaches to theoretical sloshing modelling are distinguished. One of them focuses on low-order asymptotic mathematical theories and appropriate Hamiltonian formalism for the system of ordinary differential equations governing the dominating standing waves. Another approach is based on computational fluid dynamics (CFD) [see surveys by Cariou and Casella (1999), Gerrits (2001), Celebi and Akyildiz (2002)]. The third approach deals with multimodal/pseudospectral methods. Such methods are able to provide in different versions both analytical and numerical studies and ‘build a bridge’ between the first and second ones. All three approaches have their advantages and disadvantages from mathematical, physical and engineering points of view outlined in details by the mentioned surveys. Links, common features and differences should be demonstrated. This is a difficult problem with regard to the lower-order mathematical theories (first approach) and modal/pseudospectral methods [see some details given by Faltinsen et al. (2000); Hill (2003)]. Both approaches reduce the original free boundary problem to systems of ordinary differential equations with finite nonlinear kernel and often focus on nonlinear steady state waves. The difference is that the modal methods account for the full set of activated modes and their arbitrary initial perturbation, while the first approach studies the behaviour of the leading modes. Generally speaking, the multidimensional modal approach is more general, because under some additional asymptotic assumptions (Faltinsen et al., 2000, 2003) a corresponding low-order Hamiltonian system can be derived from the modal systems. The opposite is not true. Although Hill (2003) presented a version of single-dominant theory of two-dimensional sloshing, where the behaviour of some higher modes can be restored, his scheme is invalid for arbitrary initial conditions (for the higher modes) and requires the single harmonic forcing in a very small vicinity of the primary resonance.

With the aim of capturing wide classes of forcing relevant for e.g. realistic tanks excited by ship motions the paper focuses on the modal/pseudospectral methods. Those methods can formally be separated into two branches based on *asymptotic* and *Perko-like* modal schemes (techniques). Whereas the asymptotic modal schemes (asymptotic modal methods) originated from an analytical sloshing study by Narimanov (1957), the pseudospectral Perko-like technique was first proposed by Moore and Perko (1964) and Perko (1969) for direct simulation of transient free surface flows. Both schemes assume Fourier solution of the potential flow sloshing problem in the tank-framed Cartesian coordinate system $Oxyz$ (Fig. 1) as follows:

$$f(x, y, t) = \sum_{i,j} \beta_{i,j}(t) f_{i,j}(x, y), \quad (1)$$

$$\Phi(x, y, z, t) = \mathbf{v}_0 \cdot \mathbf{P} + \boldsymbol{\omega} \cdot \boldsymbol{\Omega} + \sum_{i,j} R_{i,j}(t) \phi_{i,j}(x, y, z). \quad (2)$$

Here $z = f(x, y, t)$ is the equation of the free surface, $\Phi(x, y, z, t)$ is the velocity potential, \mathbf{v}_O and $\boldsymbol{\omega}$ are instantaneous translatory and angular velocities of the tank, $\mathbf{P} = (x, y, z)^T$, $\{f_{i,j}\}$ and $\{\varphi_{i,j}\}$ are known sets of basis functions in corresponding functional spaces, $\beta_{i,j}(t)$ and $R_{i,j}(t)$ are the unknown time-dependent functions (*modal functions*) and $\boldsymbol{\Omega}(x, y, z, t) = (\Omega_1, \Omega_2, \Omega_3)^T$ is the Stokes–Zhukovsky potential defined for instance by Faltinsen et al. (2000). The Fourier expressions (1) and (2) require vertical walls in vicinity of the mean free surface, no overturning free surface and an open tank. Further, since it implies that the free surface intersects the wall perpendicularly, it does not give an adequate description of run-up near walls. The completeness of $\{f_{i,j}\}$ and $\{\varphi_{i,j}\}$ in corresponding functional spaces (Aubin, 1972) is also needed.

The substitution of (1) and (2) into the original free boundary problem or its variational analogy (Faltinsen et al., 2000; La Rocca et al., 2000) leads to an infinite-dimensional system of nonlinear ordinary differential equations coupling the modal functions. Those systems (in truncated form) can be implemented for direct numerical simulations of fluid sloshing. This way constitutes the main idea of the Perko-like scheme (Moore and Perko, 1964; Perko, 1969). Some recent modifications of this scheme have been developed by Chern et al. (1999), La Rocca et al. (2000), Ferrant and Le Touze (2001) and Shankar and Kidambi (2002). The advantage of the Perko-like scheme relative to the asymptotic modal technique is that corresponding truncated systems of ordinary differential equations take into account the full set of high-order wave components. This makes it a promising alternative to existing CFD schemes, but not to analytical methods. Moreover, our experience shows that their implementation for large amplitude sloshing may sometimes be numerically inefficient. One difficulty is associated with the set of functions $\{\varphi_{i,j}\}$, which must be a complete Fourier basis for any admissible instantaneous fluid domain. In practice, linear natural modes of the fluid oscillations are chosen in all existing modifications of the Perko-like scheme. These modes are only a complete Fourier basis in the mean fluid domain. Even if this set of eigenfunctions can be found analytically and extended above the mean fluid surface (examples are rectangular and vertical circular cylindrical tanks), it is generally not complete for all physically possible instantaneous fluid shapes. Timokha (2002) exemplified the incompleteness for two-dimensional domains by using analytical and numerical results by Lukovsky et al. (1984). Numerical problems can also occur when the higher modes are evaluated outside the mean fluid domain. This is caused by the strong exponential character of $\{\varphi_{i,j}\}$ along the Oz -axis. Further, corresponding truncated systems of nonlinear ordinary differential equations become very stiff for larger dimensions. In contrast to Perko-like schemes the asymptotic modal technique does not provide a ‘truncation’, but rather an asymptotic reduction of the infinite-dimensional systems to a finite-dimensional form. The nondimensional forcing amplitude is assumed asymptotically small and of $\mathcal{O}(\varepsilon)$ and each modal function is ordered in terms of ε . The asymptotic scheme leads to substantial limitations of the number of higher-order nonlinear components, but the finite-dimensional asymptotic modal system reduces to a relative simple analytical structure. Corresponding simplified systems constitute the ground for analytical studies, time efficient computing and even simulations of coupling with ship motions. Recent examples are given by La Rocca et al. (1997), Faltinsen et al. (2000), Faltinsen and Timokha (2001), Gavriluk et al. (2000) and Lukovsky and Timokha (2002). Finally, the modal asymptotic schemes use the linear natural modes as a basis, but they do not require evaluation outside the mean fluid domain and are therefore not in conflict with completeness.

Asymptotic reduction of the infinite-dimensional modal systems requires an intermodal ordering, namely, relationships between the modal functions $\beta_{i,j}$ and $R_{n,k}$ (in scale ε). As a consequence, the asymptotic modal scheme suggests a preliminary physical prediction of wave phenomena. This paper emphasizes the case when the forcing frequency is very close to the lowest natural frequency. Under those resonant conditions the amplification of the lowest mode/modes should obviously be dominating and of a lower order relative to the nondimensional forcing amplitude ε . For instance, for forced sway motions the nondimensional ε is the ratio between the forcing amplitude and the horizontal length dimension of the tank along the sway direction. This type of ordering is in contrast with what is commonly done for external free surface problems, where the leading order terms are of the same order as the forcing. Further, the higher modes are in the asymptotic analysis of either higher order or of the same order as the primary dominant mode when internal resonances in this multidimensional mechanical system occur. The matching of the primary order for deep water sloshing in rectangular (two dimensional) and vertical circular cylindrical tanks was done by Moiseyev (1958) and Narimanov (1957), respectively. They showed that the lowest dominating mode should be $\mathcal{O}(\varepsilon^{1/3})$ to get nonlinear mathematically correct secular equation governing the primary amplitude response versus forcing frequency in close vicinity of the primary resonance [see also detailed description of the asymptotic detuning procedure by Ockendon and Ockendon (1973) and Faltinsen (1974)]. A corresponding asymptotic relationship is often associated with so-called Moiseyev detuning. A critical depth condition leads to loss of the third-order nonlinear component in the secular equation, so that the fifth order analysis is required (Waterhouse, 1994). In order to match shallow water asymptotics the second-order analysis is needed Ockendon et al. (1996). For the intermediate depths, Faltinsen and Timokha (2002a) showed that the asymptotic modal scheme needs fourth-order Boussinesq-type ordering, where the fluid depth is of the same order as the modal functions $\beta_{i,j}$ and $R_{n,k}$.

The asymptotic modal theory by Faltinsen et al., 2003 derived to capture nonlinear three-dimensional sloshing in a rectangular-base tank with finite depth uses Moiseyev–Narimanov-like ordering, namely only two lowest natural modes are assumed to be dominating. The present paper continues the examinations of this modal theory and presents an extensive classification of steady state waves in a square base tank by use of the asymptotic solutions obtained from the corresponding modal system. Analytical investigations are accompanied by direct numerical simulations. The theoretical predictions are validated by new experimental results for wave elevation and forces. An important finding consists in selecting frequency domains where no steady solutions exist ('chaotic' waves are expected) as well as in detecting three categories of stable steady state resonant waves for longitudinal (along the wall) and diagonal (along the diagonal of the horizontal cross-section) excitations. This has been done for a wide range of fluid depths and excitation frequencies/amplitudes. The wave types are in the first case 'planar' (two dimensional), 'swirling' [see discussion on experimental observation of 'swirling' waves in square-base tank by Barber (1969)] and 'diagonal'-like [observed earlier in experiments by Tomawa and Sueoka (1989)], and, in the second case 'diagonal', 'swirling' (see also experiments and CFD calculations by Arai et al. (1992, 1993) and 'diagonal'-like waves. The reason for generating stable 'swirling' and 'diagonal'-like wave motions for longitudinal excitations is nonlinear transfer of the energy into transversal waves caused by their small perturbations in the initial or transient phase. Since these types of motions are hydrodynamically stable, the direction of 'swirling' does not theoretically change with time and is defined exclusively by initial/random perturbations. Analogously, the initial perturbations determine along which of the two diagonals the 'diagonal'-like waves occur. Even if the planar waves due to longitudinal excitation exist in general, their effective domain is significantly influenced by three-dimensional hydrodynamic instability. This makes them in particular unstable in a narrow frequency domain around the lowest natural frequency. This domain increases with increasing excitation amplitude.

The systematization of possible steady state regimes is believed to give important guidance for CFD simulations. For instance, if CFD simulations do not show steady state behaviour, one may wrongly conclude that this is due to numerical errors. The graphs of this paper are then helpful in telling for which frequency domain, excitation amplitude and direction of forcing that 'chaotic'-type of fluid flows happens. This paper does not consider parametric waves [see survey by Perlin and Schultz (2000)] and therefore heave excitation is not studied, i.e. $v_{03} = 0$ (Fig. 1). Parametric waves are not of primary concern for the excitation frequencies that we focus on.

Although the main topic of the paper is steady state waves due to harmonic forcing, the basic modal system is believed applicable for more complicated situations. It is only restricted by the ordering of different modes, but has no limitation with regard to initial perturbations or type of excitation. Its future modifications are in part associated with an appropriate ordering of higher modes. An important consideration for that is the secondary resonances in the hydrodynamic system occurring for instance when 2σ (σ is the forcing frequency) is close to the natural frequencies $\sigma_{0,2}$, $\sigma_{2,0}$ and $\sigma_{1,1}$ or, generally, when nonlinearities cause the harmonics $n\sigma$ in the modal functions $\beta_{ij}(t)$ and $R_{n,k}(t)$ and $n\sigma \approx \sigma_{i,j}$, $i + j = n$, $h \geq 2$. The secondary resonance phenomenon is a pronounced effect for commensurate (nearly commensurate) dispersion relationships established by shallow (intermediate) fluid depths for two-dimensional sloshing (Ockendon and Ockendon, 1973; Faltinsen and Timokha, 2002a). However, even if the spectrum is not commensurate, the probability of the multiple secondary resonance for finite depths grows with increasing forcing amplitude, especially for transient waves (Bryant, 1989; Faltinsen and Timokha, 2001). The classical asymptotic scheme by Moiseyev–Narimanov employed by Faltinsen et al. (2003) does not take fully into account the secondary/internal resonances, but only predicts them for the second and third modes. Considering those predictions and the already mentioned analysis by Faltinsen and Timokha (2001) developed for two-dimensional sloshing, enables appropriate modifications of this asymptotic modal theory.

The modifications should start from assumptions that some higher modes have the same order as the primary dominant mode, i.e.

$$\beta_{ij} \sim R_{ij} = \mathcal{O}(e^{1/3}), \quad i + j \geq 1. \quad (3)$$

When relationship (3) is true for an infinite number of modes, the asymptotic infinite-dimensional modal systems (these models did not a priori specify a limited number of dominating modes) take the form equivalent to the third-order equation by Zakharov (1968), or, in a particular case, to the adaptive modal theories by Faltinsen and Timokha (2001) (two-dimensional flows). Such an infinite asymptotic modal system, where all the modes are assumed formally to contribute equally, has already been derived for three-dimensional nonlinear sloshing in rectangularly shaped tanks (Faltinsen et al., 2003, general modal system from). This general infinite system is similar to Perko-like differential models, but restricted to third-order polynomial nonlinearities. An extensive physical analysis is required to get an estimate of the number of modes having the lowest order (Faltinsen and Timokha, 2001). Some discussion on how to do that follows from our test simulations and experimental studies.

Further modifications of the modal methods should include the effect of sloshing induced slamming, i.e. roof impact. Slamming is of primary importance in design of LNG tanks. All filling heights have to be examined making roof impact important for larger depths. Since liquefied natural gas is partly boiling, the flow is in reality two-phase. Air cushions may also be created during impact. Slamming must always be considered from a structural elastic and plastic response point of view, with the possibility that hydroelasticity matters. The knowledge about physical parameters affecting slamming in LNG tanks is limited. This causes uncertainties in scaling of model tests.

2. Governing equations

The forced fluid sloshing with the mean depth h is considered in a rigid open parallelepipedal tank with breadth L_1 and width L_2 . The tank movement is described by known time-dependent vectors $v_O(t) = (v_{O1}(t), v_{O2}(t), v_{O3}(t))$ and $\omega(t) = \dot{\psi}(t) = d/dt(\psi_1(t), \psi_2(t), \psi_3(t))$ representing instantaneous translatory and angular velocities of the mobile Cartesian coordinate system $Oxyz$ relative to an absolute coordinate system $O'x'y'z'$ (Fig. 1). The fluid is perfect with irrotational flows; its motions are monitored in the mobile coordinate system $Oxyz$, which is rigidly fixed to the tank. The origin O coincides with the middle point of the mean fluid surface so that the mean fluid surface belongs to the Oxy -plane and the Ox and Oy -axes are parallel to the vertical walls. Absolute position vector $\mathbf{P}'(t) = (x', y', z')$ is decomposed into the sum of $\mathbf{P}'_O(t) = \vec{O'O}$ and the relative position vector $\mathbf{P} = (x, y, z)$. The gravity potential U depends therefore on the spatial coordinates (x, y, z) and time t , namely, $U(x, y, z, t) = -\mathbf{g} \cdot \mathbf{P}'$, $\mathbf{P}' = \mathbf{P}'_O + \mathbf{P}$, where \mathbf{g} is the gravity acceleration vector.

The mobile coordinate system is convenient to use in analysing sloshing in spacecraft and ship applications. The corresponding hydrodynamic free boundary problem is derived by Moiseyev and Rumyantsev (1968) and Narimanov et al. (1977). The problem couples the function $\zeta(x, y, z, t)$ defining the free surface evolution $\Sigma(t) : \zeta(x, y, z, t) = 0$ and the absolute velocity potential $\Phi(x, y, z, t)$ which should be determined in the time-varying volume $Q(t)$ confined to the wetted body surface $S(t)$ and $\Sigma(t)$ (Fig. 1); \mathbf{v} is the outward normal to $Q(t)$. The free boundary problem requires either initial or periodicity conditions. The initial (Cauchy) conditions require that the initial fluid shape and the initial normal velocity on the free surface are known. The periodicity conditions are associated with periodicity of wave pattern and velocity field, and are formulated for standing (free) nonlinear waves or steady state regimes caused by periodic external forcing.

2.1. Modal system

Adopting the Fourier solution of Eqs. (1) and (2) and the Luke–Bateman variational principle, Faltinsen et al. (2000) proved the equivalence of the fluid sloshing free boundary problem and an infinite-dimensional system of nonlinear ordinary differential equations coupling $\beta_{i,j}$ and $R_{n,k}$ (the modal system). In order to provide both robust computations and to be able to study analytically nonlinear sloshing it has been asymptotically simplified. Examples are given by Faltinsen et al. (2000), Faltinsen and Timokha (2001, 2002a, 2002b) (two dimensional sloshing in a rectangular tank), Gavriluk et al. (2000) (vertical circular cylinder), Lukovsky and Timokha (2002) (conical tank) and Faltinsen et al. (2003) (three-dimensional sloshing in a rectangular base tank). Our investigations that follow will be based on the last asymptotic model.

Following Faltinsen et al. (2003) we introduce dimensionless lengths, i.e. the tank has breadth 1 and width $1/r = L_2/L_1$. The original free boundary problem is then considered in nondimensional form, which suggests that the fluid depth is redefined as $h := h/L_1$ and $g := g/L_1$ (g is the gravity acceleration). The nondimensional forcing amplitudes/velocities/acceleration of sway/surge/roll/pitch excitations are assumed to be small ($\varepsilon \rightarrow 0$). This implies in particular that the nondimensional translatory forcing amplitude is small relative to L_1 and, therefore, nondimensional forcing velocities v_{O1}, v_{O2} are proportional to ε . In a similar way, the functions ψ_1, ψ_2 associated with nondimensional angular forcing are also assumed to be of order ε .

The analytical solutions $\Phi = \exp(I\sigma_{i,j}t)\varphi_{i,j}(x, y, z)$, ($I^2 = -1$) of the linearized natural sloshing problem (the natural standing waves occurring with circular frequencies $\sigma_{i,j}$) are chosen as a basis system of functions in (2), i.e.

$$\varphi_{i,j}(x, y, z) = f_i^{(1)}(x)f_j^{(2)}(y) \frac{\cosh(\lambda_{i,j}(z+h))}{\cosh(\lambda_{i,j}h)},$$

$$\lambda_{i,j} = \pi \sqrt{i^2 + r^2 j^2}, \quad \sigma_{i,j}^2 = g\lambda_{i,j} \tanh(\lambda_{i,j}h), \quad i, j \geq 0, \quad i + j \geq 1 \quad (4)$$

and

$$f_i^{(1)}(x) = \cos(\pi i(x + 1/2)), \quad i \geq 0; \quad f_j^{(2)}(y) = \cos(\pi j r(y + 1/(2r))), \quad j \geq 0. \quad (5)$$

The projections of φ_{ij} on the mean free surface $z = 0$ give the standing wave shapes $f_{ij}(x, y) = f_i^{(1)}(x)f_j^{(2)}(y) = \varphi_{ij}|_{z=0}$, $i + j \geq 1$. The set of functions $\{f_{ij}(x, y), i + j \geq 1\}$ forms an appropriate Fourier basis in the horizontal rectangular cross-section of the tank $[-1/2, 1/2] \times [-1/(2r), 1/(2r)]$ and can therefore be used in (1). The harmonic functions $\{\varphi_{ij}(x, y, z), i + j \geq 1\}$ satisfy zero-Neumann boundary conditions on the tank surface and can be adopted in (2) since the asymptotic technique requires only completeness in the unperturbed fluid domain $Q_0 = [-1/2, 1/2] \times [-1/(2r), 1/(2r)] \times [-h, 0]$, where those functions constitute the appropriate basis (Lukovsky et al., 1984; Timokha, 2002).

The paper focuses on resonant forcing of the lowest mode for finite h and $r = 1$. The pair of primary natural modes $f_1^{(1)}$ and $f_1^{(2)}$ becomes then degenerate (having equal natural frequencies) and, therefore, when the forcing frequency is close to the smallest natural frequency $\sigma_{1,0} = \sigma_{0,1} = \sigma_1$, the hydrodynamic system gives double primary resonance for the dual lowest modes with possible violent three-dimensional resonant phenomena. This is due to their synchronized periodical motions with the same frequency ('swirling' and 'diagonal'-like waves have been established in many experimental works). Nonshallow dispersion relationships (Dean and Dalrymple, 1992, $h > 0.2$) do not establish internal (secondary) resonance relationships for higher modes, namely, $\sigma_{ij} \approx 2\sigma_{1,0}$, $i + j = 2$; $\sigma_{ij} \approx 3\sigma_{1,0}$, $i + j = 3$, etc. There are therefore only two primary leading modes that are of primary concern as $\varepsilon \rightarrow 0$ and $\sigma \rightarrow \sigma_1$. The ordering of other modes can then be based on the Moiseyev–Narimanov-like asymptotic scheme, i.e.

$$\begin{aligned} \beta_{1,0} &\sim \beta_{0,1} = O(\varepsilon^{1/3}); & \beta_{2,0} &\sim \beta_{1,1} \sim \beta_{0,2} = O(\varepsilon^{2/3}), \\ \beta_{3,0} &\sim \beta_{2,1} \sim \beta_{1,2} \sim \beta_{0,3} = O(\varepsilon); \\ \beta_{i,j} &\leq O(\varepsilon), \quad i + j \geq 4. \end{aligned} \quad (6)$$

After re-denoting for brevity

$$\beta_{1,0} = a_1; \quad \beta_{2,0} = a_2; \quad \beta_{0,1} = b_1; \quad \beta_{0,2} = b_2; \quad \beta_{1,1} = c_1; \quad \beta_{3,0} = a_3; \quad \beta_{2,1} = c_{21}; \quad \beta_{1,2} = c_{12}; \quad \beta_{0,3} = b_3. \quad (7)$$

Faltinsen et al. (2003) derived the following asymptotic modal system:

$$\begin{aligned} [\ddot{a}_1 + \sigma_{1,0}^2 a_1 + d_1(\ddot{a}_1 a_2 + \dot{a}_1 \dot{a}_2) + d_2(\ddot{a}_1 a_1^2 + \dot{a}_1^2 a_1) + d_3 \ddot{a}_2 a_1 + P_{1,0}^{(1)}(\dot{v}_{01} - \tilde{S}_1 \ddot{\psi}_2 - g\psi_2)] + d_6 \ddot{a}_1 b_1^2 \\ + d_7(\ddot{b}_1 c_1 + \dot{b}_1 \dot{c}_1) + d_8 \ddot{b}_1 a_1 b_1 + d_9 \ddot{c}_1 b_1 + d_{10} \dot{b}_1^2 a_1 + d_{11} \dot{a}_1 \dot{b}_1 b_1 = 0, \end{aligned} \quad (8a)$$

$$\begin{aligned} [\ddot{b}_1 + \sigma_{0,1}^2 b_1 + d_1(\ddot{b}_1 b_2 + \dot{b}_1 \dot{b}_2) + d_2(\ddot{b}_1 b_1^2 + \dot{b}_1^2 b_1) + d_3 \ddot{b}_2 b_1 + P_{0,1}^{(2)}(\dot{v}_{02} + \tilde{S}_1 \ddot{\psi}_1 + g\psi_1)] \\ + d_6 \ddot{b}_1 a_1^2 + d_7(\ddot{a}_1 c_1 + \dot{a}_1 \dot{c}_1) + d_8 \ddot{a}_1 a_1 b_1 + d_9 \ddot{c}_1 a_1 + d_{10} \dot{a}_1^2 b_1 + d_{11} \dot{a}_1 \dot{b}_1 a_1 = 0, \end{aligned} \quad (8b)$$

$$[\ddot{a}_2 + \sigma_{2,0}^2 a_2 + d_4 \ddot{a}_1 a_1 + d_5 \dot{a}_1^2] = 0, \quad (8c)$$

$$[\ddot{b}_2 + \sigma_{0,2}^2 b_2 + d_4 \ddot{b}_1 b_1 + d_5 \dot{b}_1^2] = 0, \quad (8d)$$

$$\ddot{c}_1 + \hat{d}_1(\ddot{a}_1 b_1 + \ddot{b}_1 a_1) + \hat{d}_3 \dot{a}_1 \dot{b}_1 + \sigma_{1,1}^2 c_1 = 0, \quad (8e)$$

$$\begin{aligned} [\ddot{a}_3 + \sigma_{3,0}^2 a_3 + \ddot{a}_1(q_1 a_2 + q_2 a_1^2) + q_3 \ddot{a}_2 a_1 \\ + q_4 \dot{a}_1^2 a_1 + q_5 \dot{a}_1 \dot{a}_2 + P_{3,0}^{(1)}[\dot{v}_{01} - \tilde{S}_3 \ddot{\psi}_2 - g\psi_2]] = 0, \end{aligned} \quad (9a)$$

$$\begin{aligned} \ddot{c}_{21} + \sigma_{2,1}^2 c_{21} + \ddot{a}_1(q_6 c_1 + q_7 a_1 b_1) + \ddot{b}_1(q_8 a_2 + q_9 a_1^2) + q_{10} \ddot{a}_2 b_1 + q_{11} \ddot{c}_1 a_1 + q_{12} \dot{a}_1^2 b_1 + q_{13} \dot{a}_1 \dot{b}_1 a_1 \\ + q_{14} \dot{a}_1 \dot{c}_1 + q_{15} \dot{a}_2 \dot{b}_1 = 0, \end{aligned} \quad (9b)$$

$$\begin{aligned} \ddot{c}_{12} + \sigma_{1,2}^2 c_{12} + \ddot{b}_1(q_6 c_1 + q_7 a_1 b_1) + \ddot{a}_1(q_8 b_2 + q_9 b_1^2) + q_{10} \ddot{b}_2 a_1 + q_{11} \ddot{c}_1 b_1 + q_{12} \dot{b}_1^2 a_1 + q_{13} \dot{a}_1 \dot{b}_1 b_1 \\ + q_{14} \dot{b}_1 \dot{c}_1 + q_{15} \dot{a}_1 \dot{b}_2 = 0, \end{aligned} \quad (9c)$$

$$[\ddot{b}_3 + \sigma_{0,3}^2 b_3 + \ddot{b}_1(q_1 b_2 + q_2 b_1^2) + q_3 \ddot{b}_2 b_1 + q_4 \dot{b}_1^2 b_1 + q_5 \dot{b}_1 \dot{b}_2 + P_{0,3}^{(2)}[\dot{v}_{02} + \tilde{S}_3 \ddot{\psi}_1 + g\psi_1]] = 0, \quad (9d)$$

Table 1

Coefficients d_i and \hat{d}_i versus depth/breadth ratio h

h	d_1	d_2	d_3	d_4	d_5	d_6	d_7	d_8	d_9	d_{10}	d_{11}	\hat{d}_1	\hat{d}_3
0.3	3.290	4.551	-0.488	-41.266	-5.533	0.512	1.157	5.447	-0.120	4.935	1.025	-0.401	-4.668
0.4	3.183	3.414	-0.256	-0.595	-4.290	-0.589	1.335	4.346	0.159	4.935	-1.177	0.500	-3.195
0.5	3.153	2.933	-0.136	-0.295	-3.721	-1.040	1.441	3.895	0.303	4.935	-2.079	0.914	-2.511
0.6	3.145	2.706	-0.072	-0.152	-3.441	-1.245	1.500	3.690	0.378	4.935	-2.490	1.110	-2.180
0.7	3.143	2.592	-0.039	-0.079	-3.299	-1.344	1.533	3.591	0.417	4.935	-2.688	1.205	-2.014
0.8	3.142	2.533	-0.021	-0.042	-3.225	-1.393	1.550	3.541	0.438	4.935	-2.787	1.253	-1.931
0.9	3.142	2.502	-0.011	-0.022	-3.186	-1.418	1.560	3.516	0.448	4.935	-2.837	1.276	-1.887
1.0	3.142	2.486	-0.006	-0.012	-3.165	-1.431	1.565	3.503	0.454	4.935	-2.863	1.288	-1.865
1.1	3.142	2.477	-0.003	-0.006	-3.154	-1.438	1.568	3.497	0.457	4.935	-2.876	1.295	-1.853
1.2	3.142	2.473	-0.002	-0.003	-3.148	-1.441	1.569	3.493	0.458	4.935	-2.883	1.298	-1.847
1.3	3.142	2.470	-0.001	-0.002	-3.145	-1.443	1.570	3.491	0.459	4.935	-2.887	1.299	-1.844
1.4	3.142	2.469	0.000	-0.001	-3.143	-1.444	1.570	3.491	0.460	4.935	-2.889	1.300	-1.842
1.5	3.142	2.468	0.000	-0.001	-3.143	-1.445	1.571	3.490	0.460	4.935	-2.890	1.301	-1.841
1.6	3.142	2.468	0.000	0.000	-3.142	-1.445	1.571	3.490	0.460	4.935	-2.890	1.301	-1.841
1.7	3.142	2.468	0.000	0.000	-3.142	-1.445	1.571	3.490	0.460	4.935	-2.890	1.301	-1.841
1.8	3.142	2.468	0.000	0.000	-3.142	-1.445	1.571	3.490	0.460	4.935	-2.891	1.301	-1.840
1.9	3.142	2.467	0.000	0.000	-3.142	-1.445	1.571	3.489	0.460	4.935	-2.891	1.301	-1.840
2.0	3.142	2.467	0.000	0.000	-3.142	-1.445	1.571	3.489	0.460	4.935	-2.891	1.301	-1.840

where coefficients $d_i(h)$, $\hat{d}_i(h)$, $q_i(h)$, $P_{ij}^{(k)}(h)$ and $\tilde{S}_i(h)$ are functions of the mean fluid depth h and can be calculated prior to use (8c) (9a). The higher modes are governed by linear equations

$$\ddot{\beta}_{i,j} + \sigma_{ij}\beta_{i,j} + P_{ij}^{(2)}[\dot{v}_{02} + \tilde{S}_j\ddot{\psi}_1 + g\psi_i] + P_{ij}^{(1)}[\dot{v}_{01} - \tilde{S}_i^{(1)}\dot{\psi}_2 - g\psi_2] = 0, i + j \geq 4. \tag{10}$$

We recognize in (8c) and (9a) that the terms in square brackets are associated with ‘planar’ flows in either Oxz or Oyz planes; they are exactly the same as derived by Faltinsen et al. (2000). The natural frequencies σ_{ij} are governed by (4), while

$$\tilde{S}_i = \frac{2}{\pi i} \tanh(\pi i h / 2); \quad P_{ij}^{(1)} = \frac{2\delta_{0j} E_{i,0}}{(\pi i)^2} [(-1)^i - 1]; \quad P_{ij}^{(2)} = P_{j,i}^{(1)}.$$

The formulae for nondimensional coefficients $d_i(h)$, $\hat{d}_i(h)$ and $q_i(h)$ are explicitly given by Faltinsen et al. (2003) (for pure square geometry $d_{12} = d_7$ and $\hat{d}_2 = \hat{d}_1$ in their definitions). They are of relatively complicated structure. In order to facilitate computations by interested readers we give in Tables 1, and 2 the values of d_i , \hat{d}_i and q_i for different depths $h \geq 0.3$. Readers can interpolate them for intermediate values of h or, when accurate calculations are required, code the original formulae from Faltinsen et al. (2003) (comparison of these calculations with the tables becomes then an additional numerical control). Note, that dimensional values of the wave elevations can easily be computed by multiplying each modal function by L_1 .

Fig. 2 illustrates the modes involved in the nonlinear interaction. Here the first row corresponds to the primary modes of $\mathcal{O}(\varepsilon^{1/3})$, the second row describes the free surface shapes of the second-order modes of $\mathcal{O}(\varepsilon^{2/3})$ and the last row presents four modes of $\mathcal{O}(\varepsilon)$. The first and the second columns present the modes corresponding to the two-dimensional waves. In addition, since $\sigma_{0,1} = \sigma_{1,0}$ the primary modes may perform synchronized cosine-like oscillations leading to ‘diagonal’ flows. In order to capture those ‘diagonal’ flows we introduce also the auxiliary modes

$$S_1^i(x, y) = f_i^{(1)}(x) - f_i^{(2)}(y); \quad S_2^i(x, y) = f_i^{(1)}(x) + f_i^{(2)}(y) \tag{11}$$

recombining two Stokes modes of (5) into three-dimensional patterns (see the framed patterns in Fig. 2). These will be denoted as ‘diagonal’ or [due to Miles (1994)] ‘square’. If different nonzero weight coefficients are associated with $f_i^{(1)}$ and $f_i^{(2)}$, i.e. $Af_i^{(1)} + Bf_i^{(2)}$, $AB \neq 0$, $|A| \neq |B|$, we call them ‘diagonal’-like (‘square’-like) modes.

Table 2
Coefficients q_i versus depth/breadth ratio

h	q_1	q_2	q_3	q_4	q_5	q_6	q_7	q_8	q_9	q_{10}	q_{11}	q_{12}	q_{13}	q_{14}	q_{15}
0.3	-1.720	2.379	-0.255	23.168	-13.310	-0.856	5.446	2.554	6.600	0.241	-0.420	6.956	34.705	-8.451	-4.026
0.4	-0.836	0.896	-0.067	13.827	-11.221	-0.208	0.923	3.279	4.128	0.608	-0.041	-0.614	20.529	-6.808	-3.088
0.5	-0.426	0.397	-0.018	10.387	-10.313	0.081	-0.601	3.587	3.213	0.706	0.095	-3.131	15.305	-6.098	-2.720
0.6	-0.223	0.191	-0.005	8.883	-9.880	0.221	-1.208	3.732	2.826	0.732	0.146	-4.123	13.080	-5.769	-2.558
0.7	-0.117	0.097	-0.001	8.163	-9.662	0.292	-1.477	3.804	2.650	0.739	0.167	-4.557	12.051	-5.609	-2.481
0.8	-0.062	0.050	0.000	7.800	-9.550	0.329	-1.604	3.842	2.567	0.741	0.175	-4.761	11.552	-5.529	-2.442
0.9	-0.033	0.026	0.000	7.612	-9.491	0.349	-1.666	3.861	2.526	0.741	0.178	-4.860	11.303	-5.488	-2.422
1.0	-0.018	0.014	0.000	7.514	-9.460	0.359	-1.698	3.871	2.505	0.742	0.179	-4.910	11.176	-5.468	-2.412
1.1	-0.009	0.007	0.000	7.461	-9.444	0.365	-1.714	3.877	2.495	0.742	0.180	-4.936	11.110	-5.457	-2.406
1.2	-0.005	0.004	0.000	7.434	-9.435	0.367	-1.722	3.880	2.489	0.742	0.180	-4.949	11.076	-5.451	-2.403
1.3	-0.003	0.002	0.000	7.419	-9.430	0.369	-1.726	3.881	2.487	0.742	0.180	-4.956	11.058	-5.448	-2.402
1.4	-0.001	0.001	0.000	7.411	-9.428	0.370	-1.729	3.882	2.485	0.742	0.180	-4.959	11.049	-5.447	-2.401
1.5	-0.001	0.001	0.000	7.407	-9.426	0.370	-1.730	3.883	2.484	0.742	0.180	-4.961	11.044	-5.446	-2.400
1.6	0.000	0.000	0.000	7.405	-9.426	0.371	-1.730	3.883	2.484	0.742	0.180	-4.962	11.042	-5.445	-2.400
1.7	0.000	0.000	0.000	7.404	-9.425	0.371	-1.731	3.883	2.484	0.742	0.180	-4.963	11.040	-5.445	-2.400
1.8	0.000	0.000	0.000	7.403	-9.425	0.371	-1.731	3.883	2.484	0.742	0.180	-4.963	11.039	-5.445	-2.400
1.9	0.000	0.000	0.000	7.403	-9.425	0.371	-1.731	3.883	2.484	0.742	0.180	-4.963	11.039	-5.445	-2.400
2.0	0.000	0.000	0.000	7.402	-9.425	0.371	-1.731	3.883	2.484	0.742	0.180	-4.963	11.039	-5.445	-2.400

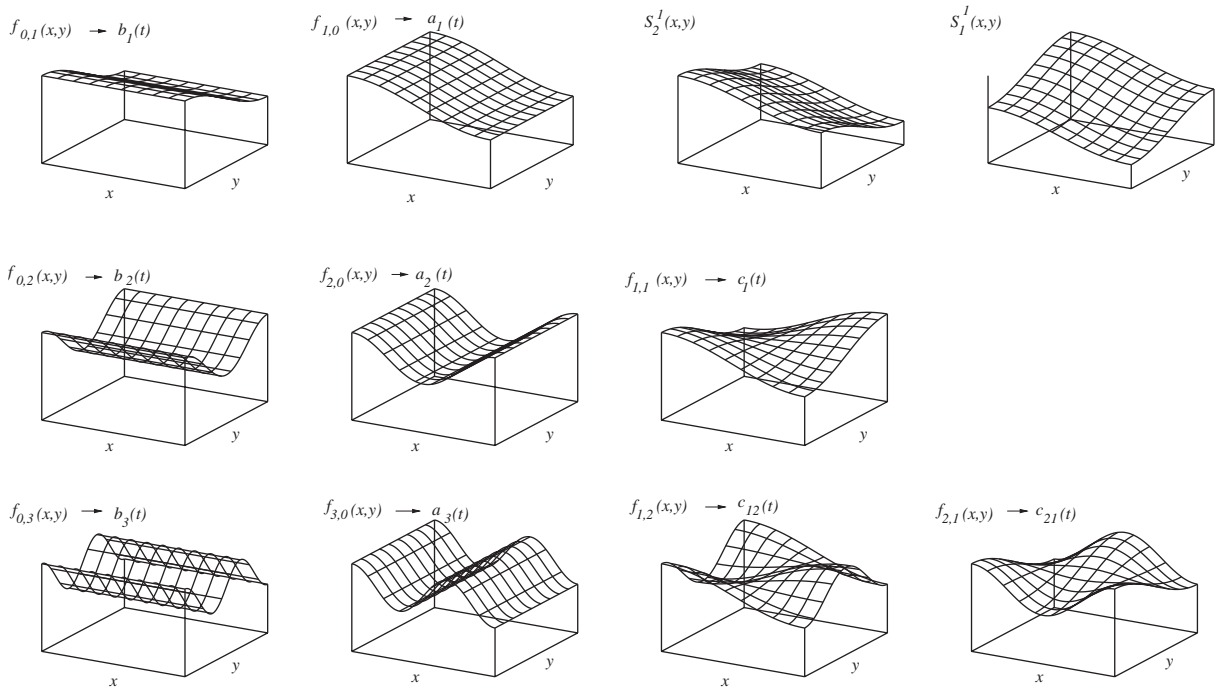


Fig. 2. The modal wave patterns associated with the natural modes that are involved in nonlinear interaction for sloshing in a square-base tank with finite depth.

System (8)–(10) needs the initial conditions

$$\begin{aligned}
 a_1(0) &= a_1^0, \quad \dot{a}_1(0) = a_1^1, \quad \dots, \quad b_3(0) = b_3^0, \quad \dot{b}_3(0) = b_3^1, \\
 \beta_{i,j} &= \alpha_{i,j}^0; \quad \dot{\beta}_{i,j} = \alpha_{i,j}^1, \quad i + j \geq 4,
 \end{aligned}
 \tag{12}$$

where the known constants $a_1^0, \dots, b_3^1, \alpha_{ij}^0$ and α_{ij}^1 describe initial free surface shape and the initial free surface velocity. For periodic forcing one can also define periodic conditions.

2.2. Hydrodynamic force

Lukovsky (1990) gives a convenient formula for calculation of the hydrodynamic force acting on the tank as follows

$$\mathbf{F} = (F_x, F_y, F_z)^T = mL_1 \mathbf{g} - mL_1 [\dot{\mathbf{v}}_O + \boldsymbol{\omega} \times \mathbf{v}_O + \boldsymbol{\omega} \times (\boldsymbol{\omega} \times \mathbf{r}_C) + \dot{\boldsymbol{\omega}} \times \mathbf{r}_C + 2\boldsymbol{\omega} \times \dot{\mathbf{r}}_C + \ddot{\mathbf{r}}_C]. \tag{13}$$

Here m is the fluid mass and \mathbf{r}_C is the nondimensional radius-vector of the centre of mass in the moving coordinate system. This formula has mathematically been derived by using the original definition of the hydrodynamic force as $\mathbf{F} = \int_{S(t)} p(x, y, z, t) \mathbf{v} dS$, where p is the pressure. The terms of (13) allow favourable physical interpretation as given by Faltinsen and Timokha (2001), namely, $mL_1 \mathbf{g}$ is the fluid weight and the terms in square brackets mean: $\dot{\mathbf{v}}_O$ is the acceleration of the origin O , $\boldsymbol{\omega} \times \mathbf{v}_O$ is the tangential acceleration, $\boldsymbol{\omega} \times (\boldsymbol{\omega} \times \mathbf{r}_C)$ is the centripetal acceleration, $2\boldsymbol{\omega} \times \dot{\mathbf{r}}_C$ is the Coriolis acceleration, $\ddot{\mathbf{r}}_C$ is the relative acceleration.

Accounting for the smallness of nondimensional forcing, the formula ($\psi_i \sim v_{O_i} \sim \varepsilon$), Eq. (13), reduces to

$$\begin{cases} F_x = mL_1(g\psi_1 - \dot{v}_{Ox} + \frac{1}{2}\dot{\omega}_2 - \ddot{x}_C + \mathcal{O}(\varepsilon)), \\ F_y = mL_1(-g\psi_2 - \dot{v}_{Oy} - \frac{1}{2}\dot{\omega}_1 - \ddot{y}_C + \mathcal{O}(\varepsilon)), \\ F_z = mL_1(-g - \ddot{z}_C + \mathcal{O}(\varepsilon)), \end{cases} \tag{14}$$

where \mathbf{r}_C are calculated as

$$\begin{cases} x_C = -\frac{2}{\pi^2 h} \left[a_1 + \frac{a_3}{9} \right], \\ y_C = -\frac{2}{\pi^2 h r} \left[b_1 + \frac{b_3}{9} \right], \\ z_C = -\frac{h}{2} + \frac{1}{4h} (a_1^2 + b_1^2 + 2(a_1 a_2 + b_1 b_2)). \end{cases} \tag{15}$$

3. Model tests

A series of model tests on resonant sloshing has been conducted to establish the resonant steady state wave motions. The experiments were accompanied by both video recordings and actual measurements of the free surface elevations near the walls at the wave probes as indicated in Fig. 3. The tank had a square base with breadth/width 59 cm and a height of 80 cm. The tank height was sufficiently large to avoid tank roof impact due to sloshing in the documented series. It was ensured that the walls and bottom of the tank were stiff enough to avoid hydroelastic effects. Fresh water was used. The nondimensional water depths were $h = 0.508, 0.34$ and 0.27 . The set-up allowed changes in the excitation direction. The majority of the experiments were done for horizontal longitudinal (along the Ox -axis) and diagonal excitations as indicated on the top view in Fig. 3. Only translatory forced tank motions are considered. However, the mathematical expressions for the pitch and roll excitations are similar and can be easily studied. The forced tank velocity is expressed as $\dot{v}_{O_i} = -\sigma^2 H_i \cos \sigma t$ with

$$H_1 = H \cos \theta_1, \quad H_2 = H \sin \theta_1$$

($H = \varepsilon$ is the amplitude of translatory excitation). Two excitation directions are considered, i.e. $\theta_1 = 0$ (longitudinal excitations) and $\theta_1 = \pi/4$ (diagonal excitations).

The typical dimensional excitation amplitude was about 0.5 cm. This means nondimensional value $H = 0.0078$ for longitudinal forcing and $H_1 = 0.0078/\sqrt{2}, H_2 = 0.0078/\sqrt{2}$ for diagonal excitations. A few measurements were made with higher forcing amplitudes $H = 0.025$ (for longitudinal excitations only). The wave probes 1–6 were of two different types (Fig. 3). Numbers 1 and 6 are made of thin wires with 0.5 mm diameter and placed a distance 40 mm from the wall. The experimental error due to meniscus effects for wave probes 1 and 6 is less than 1 mm. The other probes are made of copper tape. They are placed directly on the tank walls and have a total width of approximately 20 mm. Since experiments were done prior to theoretical studies and the authors were not familiar with possible theoretical predictions, the test series were done for a wide range of excitation frequencies in the vicinity of primary resonance ($0.86 < \sigma/\sigma_1 < 1.08, \sigma_1 = \sigma_{0,1} = \sigma_{1,0}$). The horizontal forces along the Ox and Oy -axes have also been measured.

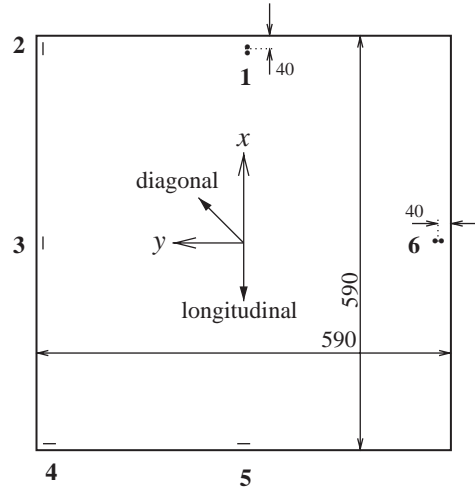


Fig. 3. The top view of the tank with positions of the wave probes. All the numbers in mm.

The experimental series are approximately 120 s long. This corresponds to 100–130 forcing periods for different time series. Due to importance of transients, only the last 30–50 s of measurements might under certain circumstances be used to indicate what type of steady state motions were achieved. Since video recordings demonstrated a significant run-up in terms of a thin film of water at the wall, only wave probes 1 and 6 placed at a small distance from the wall were used in the analysis.

4. Classification and validation

The theoretical classification of the nonlinear free surface waves is related to stable resonant steady state regimes occurring due to harmonic forcing with the excitation frequency close to the primary resonance ($\sigma \rightarrow \sigma_{1,0} = \sigma_{0,1} = \sigma_1$ in our case). Faltinsen et al. (2003) obtained analytically the third-order asymptotic steady state solution of the modal system accounting for the terms up to $\mathcal{O}(\varepsilon)$. These solutions exist, if and only if, four primary amplitudes A, \bar{A}, \bar{B}, B of the dominating modes

$$a_1(t) = A \cos \sigma t + \bar{A} \sin \sigma t + \mathcal{O}(\varepsilon^{1/3}); \quad b_1(t) = \bar{B} \cos \sigma t + B \sin \sigma t + \mathcal{O}(\varepsilon^{1/3}) \quad (16)$$

satisfy the following secular system of nonlinear algebraic equations:

$$\begin{cases} A(m_0 + m_1(A^2 + \bar{A}^2) + m_2\bar{B}^2 + m_3B^2) + (m_2 - m_3)\bar{A}\bar{B}B = P_1H_2, \\ \bar{A}(m_0 + m_1(A^2 + \bar{A}^2) + m_2B^2 + m_3\bar{B}^2) + (m_2 - m_3)A\bar{B}\bar{B} = 0, \\ \bar{B}(m_0 + m_1(B^2 + \bar{B}^2) + m_2A^2 + m_3\bar{A}^2) + (m_2 - m_3)\bar{A}A\bar{B} = P_1H_2, \\ B(m_0 + m_1(B^2 + \bar{B}^2) + m_2\bar{A}^2 + m_3A^2) + (m_2 - m_3)\bar{A}A\bar{B} = 0, \end{cases} \quad (17)$$

where $P_1 = P_{0,1}^{(2)} = P_{1,0}^{(1)}$ and the coefficients m_0, m_1, m_2 and m_3 are functions of σ and h . Taking into account the ordering of $A, \bar{A}, \bar{B}, B = \mathcal{O}(\varepsilon^{1/3})$ and $H = \mathcal{O}(\varepsilon)$ gives $m_0 = \mathcal{O}(\varepsilon^{2/3})$ and $m_i = \mathcal{O}(1)$ in the secular system in order to keep the terms up to $\mathcal{O}(\varepsilon)$. Under the resonant condition $(\sigma - \sigma_1) \ll 1$ we need only $m_i = m_i|_{\sigma=\sigma_1}(h)$, $i \geq 1$ in (17) to satisfy that. The solvability of Eq. (17) can then be studied for different h . Analysis by Faltinsen et al. (2003) showed that the secular system may have either no solutions for some isolated critical depths, or multiple solutions which appear/disappear or change the system behaviour for other critical depths or infinite solutions for $\sigma \rightarrow \sigma_1$. One of those critical depths $h_1 = 0.337 \dots$ is related to change from soft to hard spring type of the ‘planar’ waves [see two-dimensional analysis by Fultz (1962), Waterhouse (1994), Faltinsen et al. (2000)]. Other critical depths are connected exclusively with three-dimensional resonant regimes. They are mathematically defined and calculated by Faltinsen et al. (2003) and we refer interested readers to this work. That paper provides also the stability analysis for steady state solutions by using the first Lyapunov scheme. This makes it possible in the section below to classify possible stable resonant waves for finite depths ($h > 0.2$).

4.1. Longitudinal excitations

Three possible resonant steady state waves for longitudinal excitation are best described in terms of the primary amplitudes (A is always nonzero), i.e.

(i) ‘planar’

$$f(x, y, t) = Af_1^{(1)}(x) \cos \sigma t + \mathcal{O}(\varepsilon^{1/3}), \tag{18}$$

occurring when $A \neq 0$ and $\bar{A} = B = \bar{B} = 0$,

(ii) ‘diagonal’-like

$$f(x, y, t) = [Af_1^{(1)}(x) \pm \bar{B}f_1^{(2)}(y)] \cos \sigma t + \mathcal{O}(\varepsilon^{1/3})$$

$$= \left[A_1^\pm \underbrace{(f_1^{(1)}(x) - f_1^{(2)}(y))}_{S_1^1(x,y)} + B_1^\pm \underbrace{(f_1^{(1)}(x) + f_1^{(2)}(y))}_{S_2^1(x,y)} \right] \cos \sigma t + \mathcal{O}(\varepsilon^{1/3}) \tag{19}$$

occurring for $A \neq 0$ and $\bar{A} = B = 0$, $\bar{B} \neq 0$, and, finally,

(iii) ‘swirling’

$$f(x, y, t) = Af_1^{(1)}(x) \cos \sigma t \pm Bf_1^{(2)}(y) \sin \sigma t + \mathcal{O}(\varepsilon^{1/3}) \tag{20}$$

occurring for $A \neq 0$ and $B \neq 0$, $\bar{B} = \bar{A} = 0$. The reason why (20) describes ‘swirling’ is that the x - and y -dependent terms are 90° out of phase. The \pm ahead of amplitude component B in (20) means clockwise or counterclockwise ‘rotation’. Since a ‘diagonal’-like wave corresponds to a nearly diagonal standing wave, \pm in (19) describes the possibility that the waves can occur approximately along either of the two diagonals. Both signs are mathematically possible. This means that initial conditions and transient phase will determine the sign.

New results on distribution of effective frequency domains in the $(\sigma/\sigma_1, h)$ -plane are presented in Figs. 4(a–d) for four different forcing amplitudes, $0.2 < h < 0.6$ and $0.85 < \sigma/\sigma_1 < 1.15$. The arrows indicate the region of stable steady state motions (the corresponding steady regimes disappear/become unstable in the direction of the arrows). Figs. 4 (a–d) show that the region of stable planar waves is always away from the primary resonance $\sigma/\sigma_1 = 1$. The region where planar waves are unstable is denoted as $D_2D_4FGEO_2O_1$. Figs. 4 (a–d) demonstrate that this region becomes wider with increasing forcing amplitude. It should be noted that two-dimensional analysis Faltinsen (1974) does not give any instability region. This means that this instability is caused by three-dimensional wave perturbations.

Geometrically, $D_2D_4FGEO_2O_1$ falls into three sub-regions, i.e. O_1CGEO_2 corresponds to stable ‘diagonal’-like waves (these waves are absent for deep water and $\sigma/\sigma_1 \approx 1$), FD_4D_3 corresponds to stable ‘swirling’ waves (it disappears at $\sigma/\sigma_1 = 1$ for small depths) and D_2D_3FEC implies no stable steady state solution (this region also disappears for small depths). The last region is often associated in dynamic systems with ‘chaotic’ motions. Away from the region $D_2D_4FGEO_2O_1$ the planar waves may co-exist with either ‘swirling’ (R_1FD_4) or ‘diagonal’-like waves ($ABCD_1$). There are no regions where stable ‘swirling’ waves co-exist with stable ‘diagonal’-like waves. The domain of stable ‘swirling’ drifts right of the resonant zone for sufficiently small h , while the effective domain of stable ‘diagonal’-like waves drifts left of the main resonance for sufficiently large depths (deep water). Note that increasing forcing amplitude does not change qualitatively the distribution of the frequency domains with different types of wave motions.

The theoretical results were experimentally validated for the case $H = 0.0078$. Fig. 4(c) illustrates good qualitative agreement in this case, especially for $h = 0.508$. For smaller depths the experiments show a reduction and a shift of the ‘chaotic’ region relative to the theoretical prediction. This tendency is illustrated by experimental series with $h = 0.34$. When decreasing depth to $h = 0.27$, the experiments show the planar waves in region D_2CEGFD_3 , but no chaotic waves are detected as are predicted by the theory. A possible explanation is the neglecting of the damping, which becomes of primary concern for smaller depths. The damping no doubt reduces the “chaotic” frequency domains. Another interesting point is that theoretical prediction suggests a slight drift to the right relative to the experimental data. Since any drifts in a “frequency-amplitude” response of a mechanical system are in most cases caused by nonlinearities, it is believed that improvements of the asymptotic modal theory should be associated with modifications of the asymptotic ordering to account for nonlinear interaction of some higher modes. This is also explicitly confirmed by both our direct numerical simulations and experiments (see the next section), which established significant contribution from nonprimary modes. This situation is similar to the one explained by Faltinsen and Timokha (2001, 2002a) for two-dimensional resonant waves.

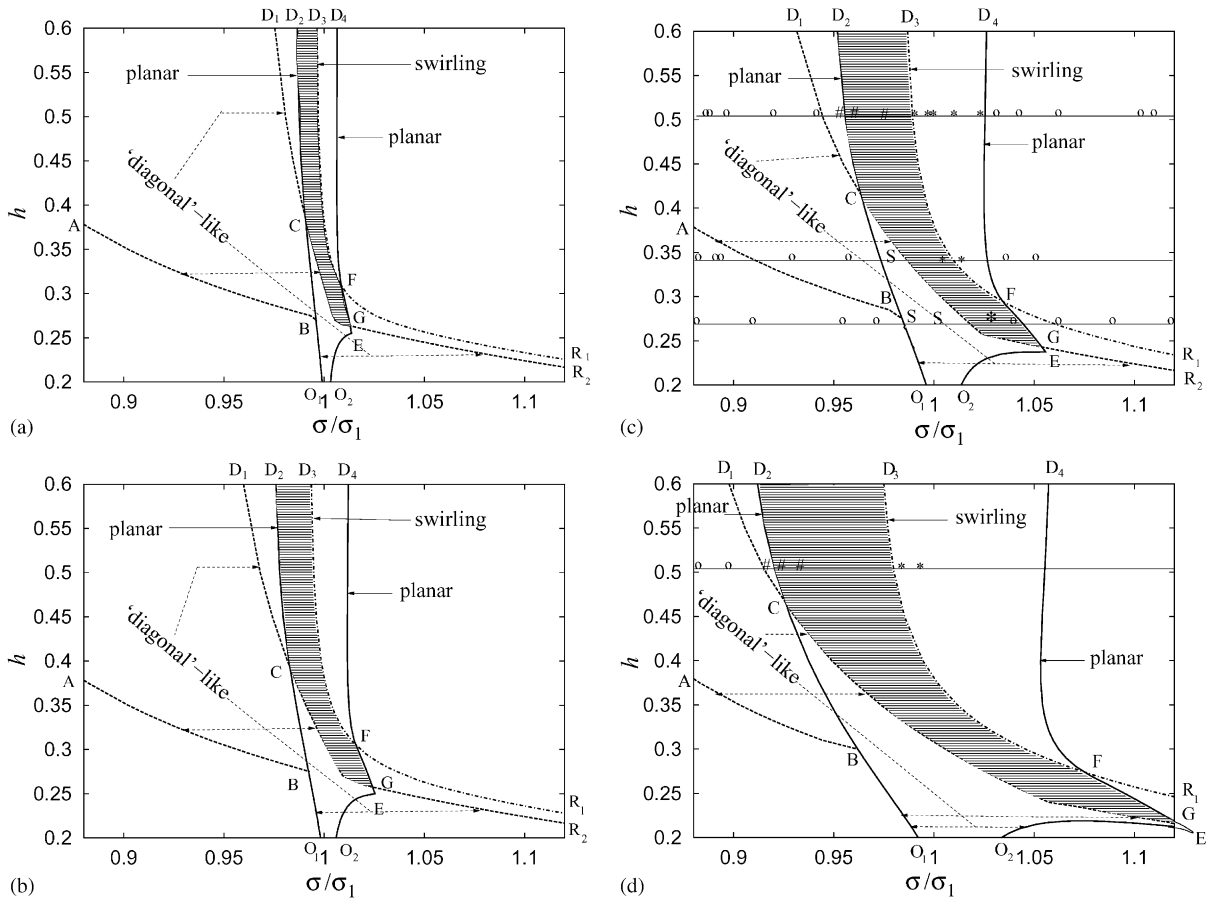


Fig. 4. Theoretical frequency domains of stable resonant steady state motions presented as function of the depth/breadth ratio h versus the ratio between the excitation frequency and the lowest natural frequency σ/σ_1 ($\sigma_1 = \sigma_{0,1}$) for different forcing amplitude/breadth ratios. Longitudinal (surge) excitations ($\theta_1 = 0$) with the following amplitudes (a) $H = 0.001$, (b) $H = 0.0025$, (c) $H = 0.0078$ and (d) $H = 0.025$. Shaded area (chaos) indicates the frequency domain, where no stable steady state waves occur. Comparisons with experimental observations are made in (c) for the fluid depths $h = 0.508, 0.34$ and 0.27 and in (d) for $h = 0.508$. Experimental data are denoted as 'o' – 'planar' waves, '*' – 'swirling' waves, '#' – 'chaos' and 'S' – 'diagonal'-like waves.

One should also note that the theory for case $h = 0.508$ predicts two frequency domains away from the primary resonance domain $\sigma/\sigma_1 = 1$ where either stable 'swirling' or 'diagonal'-like waves co-exist with 'planar' waves. Theoretically, the initial conditions determine what kind of steady state motions are realized after initial transients. In practice these initial conditions consist of small perturbations of various types. The influence of small initial/random perturbations was unavoidable in our experimental tests. Ideally, the time domain simulations with damping coefficients (see the next section) and zero-initial conditions may address this problem. However, since the system demonstrates in some cases a sensitivity to small changes of the initial conditions, which are not exactly known, qualitative arguments related to the difference in the amplitudes (energy) of co-existing stable waves are used. If there is a clear difference in amplitude and there are nearly-zero initial conditions, the steady wave system with the lowest energy is most likely to occur. The 'planar' solutions are of lower energy in both mentioned frequency domains. It is therefore most probable that 'swirling' and 'diagonal'-like wave were not physically realized in these experiments for corresponding excitation frequencies and that planar flow occurs. Since the effective frequency domain of the 'diagonal'-like solutions always co-exists with planar waves for $h = 0.508$, we were strongly motivated to find them in observations for $h = 0.34, 0.27$. Corresponding experimental observations are denoted S in Fig. 4(c) and show good agreement with theoretical predictions. The theory agrees also well with experimental data for $h = 0.508$ and the relatively large forcing amplitude presented in Fig. 4(d).

4.2. Diagonal excitations

Faltinsen et al. (2003) found three and only three periodic resonant waves for the diagonal harmonic excitations (treated in terms of ‘diagonal’ modes), i.e.

- (i) ‘diagonal’ waves (the pure diagonal (square) mode $S_2^1(x, y)$ is nonlinearly excited)

$$f = B_1 S_2^1(x, y) \cos \sigma t + \mathcal{O}(\varepsilon^{1/3}) \quad (21)$$

occurring for $B = -\bar{A} = 0$, $A = \bar{B} \stackrel{\text{def}}{=} B_1$,

- (ii) ‘diagonal’-like waves

$$f = [\pm A_1 S_1^1(x, y) + B_1 S_2^1(x, y)] \cos \sigma t + \mathcal{O}(\varepsilon^{1/3}) \quad (22)$$

describing joint cosine amplification of the pair S_1^1 and S_2^1 (here $B_1 \stackrel{\text{def}}{=} (A + \bar{B})/2$, $A_1 \stackrel{\text{def}}{=} (A - \bar{B})/2$) occurring for $B = -\bar{A} = 0$, $A \neq \bar{B}$, and, finally

- (iii) ‘swirling’ waves

$$f = B_1 S_2^1(x, y) \cos \sigma t \mp A_1 S_1^1(x, y) \sin \sigma t + \mathcal{O}(\varepsilon^{1/3}) \quad (23)$$

occurring for $A_1 \stackrel{\text{def}}{=} \bar{A} = -B \neq 0$, $B_1 \stackrel{\text{def}}{=} A = \bar{B}$.

Figs. 5(a–d) demonstrate the effective frequency domain for the resonant stable steady state waves due to diagonal excitation. The figures present the change of the frequency domains for $0.2 < h < 0.6$ and $0.9 < \sigma/\sigma_1 < 1.1$ with different excitation amplitudes. The calculations establish relatively narrow regions of ‘chaotic’ waves (no stable steady state regimes occur). One of these regions $T_2 T_3 F$ is found for $0.5 \lesssim h$. For smaller depths ($h < 0.3$) the corresponding region is zoomed in Figs. 5(a–c). The last range is probably too small and should be reduced by even smaller damping. In addition, the numerical analysis captures a zone D for small depths ($h \leq 0.27$) where diagonal steady state nonlinear waves are always stable. This frequency domain decreases with increasing forcing amplitude. When $h > 0.3$, Figs. 5(a–d) show no stable ‘diagonal’-like waves. However, two finger-like areas of stable ‘diagonal’-like waves are established for smaller depths. These become wider for relatively large excitation amplitudes (Figs. 5(c,d)). Another interesting point is that two different stable steady regimes (‘diagonal’ and ‘swirling’) co-exist for $h > 0.27$ in vicinity of the main resonance $\sigma/\sigma_1 = 1$. This can be realized due to different transient/initial perturbation scenarios causing either ‘diagonal’ or ‘swirling’ waves.

Theoretical results on resonant sloshing due to diagonal excitations were compared with experimental wave data for $h = 0.508, 0.34$ and $H = 0.0078$ (Fig. 5(c)). There is generally good agreement except for the points denoted by ‘?’. These points correspond to the fact that two theoretically predicted steady state motions (‘diagonal’ and ‘swirling’) co-exist and have approximately equal energy. This means that both types of periodical solutions are physically and mathematically possible when starting from planar initial free surface shape. The measurements show regular ‘beating’ waves in this zone. We cannot based on this conclude which stable periodic solution will be realized from zero-initial conditions. This would require a much longer time series. In addition, we cannot mathematically ignore possible stable steady state aperiodic waves. Additional theoretical and experimental investigations of this phenomenon are needed.

5. Time domain simulations and validation

5.1. Damping

Although the experiments showed that dissipation is not significant for nonsmall depths, we made some efforts to account for it. This was done in a similar way as described by Faltinsen and Timokha (2002a) for low viscosity fluid (large Galileo numbers) and two-dimensional flows. The method relates the damping to linear logarithmic decrements $\alpha_{i,j}$ calculated for each natural mode in free linear sloshing regimes. These damping rates are constant values in the framework of the linear sloshing theory and can be taken into account by the modal system by incorporating the linear terms $2\alpha_{i,j}\hat{\beta}_{i,j}$ in corresponding differential equations with index i, j , $i + j \geq 1$. In general, the damping rates $\alpha_{i,j}$ express the sum of different types of energy dissipation, namely,

$$\alpha_{i,j} = \alpha_{i,j}^{\text{bulk}} + \alpha_{i,j}^{\text{surface}} + \alpha_{i,j}^{\text{other}}, \quad (24)$$

where $\alpha_{i,j}^{\text{bulk}}$ is the dissipation due to viscosity of the fluid bulk and $\alpha_{i,j}^{\text{surface}}$ is the boundary layer dissipation on the wetted tank surface. By generalizing the derivations by Keulegan (1959) [see also the original formula (25.6) by Landau and

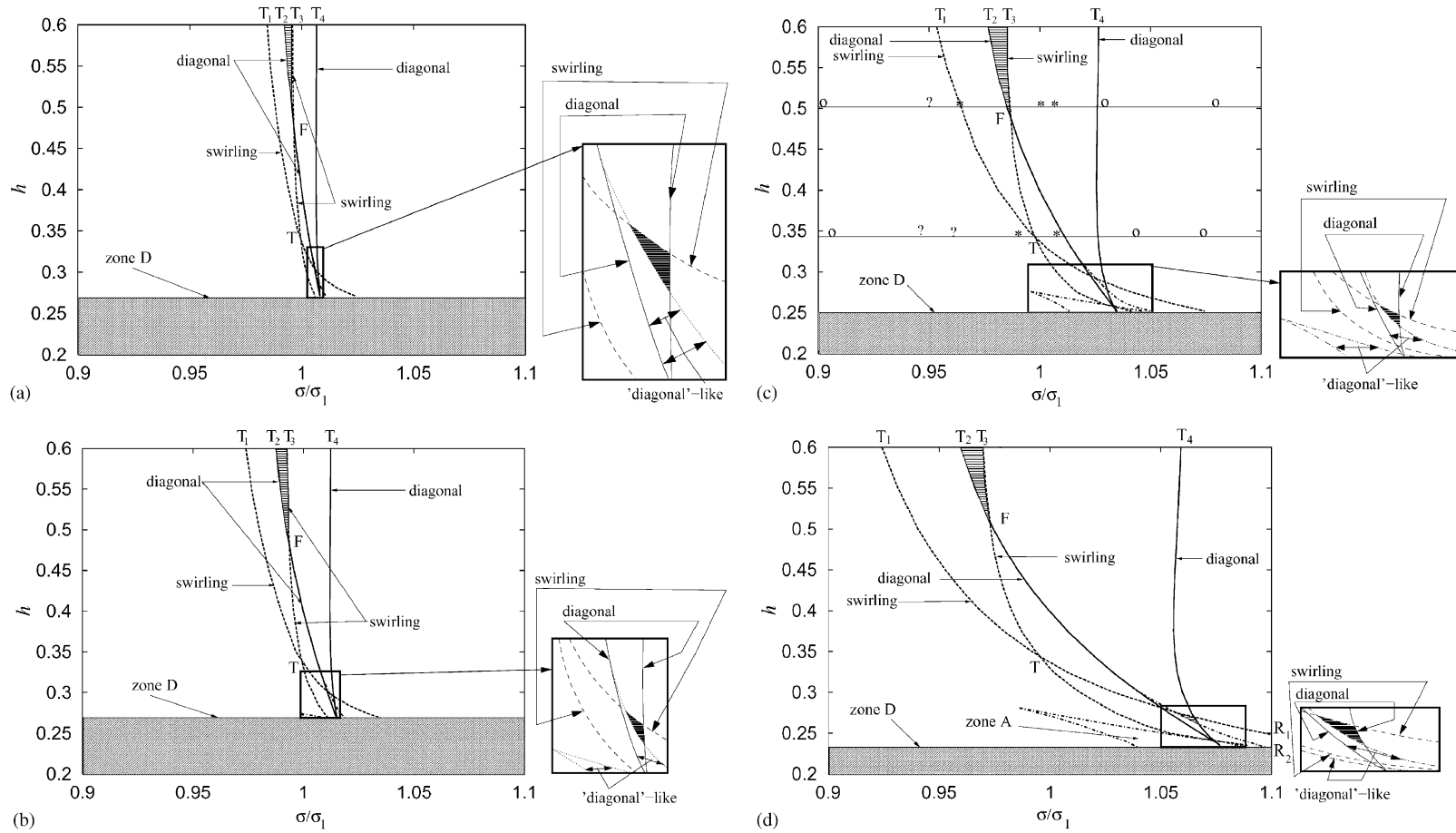


Fig. 5. Theoretical frequency domains of stable resonant steady state motions presented as function of the depth/breadth ratio h versus the ratio between the excitation frequency and the lowest natural frequency σ/σ_1 ($\sigma_1 = \sigma_{0,1}$) for different forcing amplitude/breadth ratios. Diagonal excitations ($\theta_1 = \pi/4$) with the following amplitudes (a) $H = 0.001$, (b) $H = 0.0025$, (c) $H = 0.0078$ and (d) $H = 0.025$. Shaded area (chaos) indicates the frequency domain, where no stable steady-state waves occur. Comparisons with experimental observations are made in (c) for the fluid depths $h = 0.508$ and 0.34 . Experimental data are denoted as 'o' – 'diagonal' waves, '*' – 'swirling', '# – 'chaos', 'S' – 'diagonal'-like and '?' – regular beating.

Lifshitz (1987) for the dissipation on a plate] done for two-dimensional flows with finite depths to three-dimensional sloshing in a square base tank we get

$$\alpha_{i,j}^{\text{surface}} = \sqrt{\frac{\nu\sigma_{i,j}}{2}} \left[\frac{3}{2} + \frac{\lambda_{i,j}}{\sinh(2\lambda_{i,j}h)} \left(\frac{1}{2} - h \right) \right], \tag{25}$$

where ν is the nondimensional kinematic viscosity.

Further, by following Landau and Lifshitz (1987) (example 2 below paragraph 25) we get

$$\alpha_{i,j}^{\text{bulk}} = 2\nu \left[\left(\frac{\pi^4(ij)^2}{\lambda_{i,j}^2} + \lambda_{i,j}^2 \right) + \frac{2h\pi^4(ij)^2 - \lambda_{i,j}^4}{\lambda_{i,j}\sinh(2\lambda_{i,j}h)} \right]. \tag{26}$$

The values $\alpha_{i,j}^{\text{other}}$ are for instance due to overturning and wave spilling breaking. This effect cannot be analytically estimated and our calculations assumed $\alpha_{i,j}^{\text{other}} = 0$ to avoid speculation.

5.2. Direct numerical simulations

We incorporated the terms $2\alpha_{1,0}\dot{a}_1, 2\alpha_{0,1}\dot{b}_1, \dots, 2\alpha_{i,j}\dot{\beta}_{i,j}, i + j \geq 4$ with viscous damping rates into the modal system (8)–(10) and used it for direct numerical simulations of steady state regimes. Since the simulations required the initial conditions (12), two physical scenarios were tested. The first scenario assumed initially unperturbed fluid (zero-initial conditions). If the steady state response is stable, the small viscous damping should theoretically lead to steady state conditions after a long time series. The second scenario assumes that pre-simulated sloshing has already led to a nearly

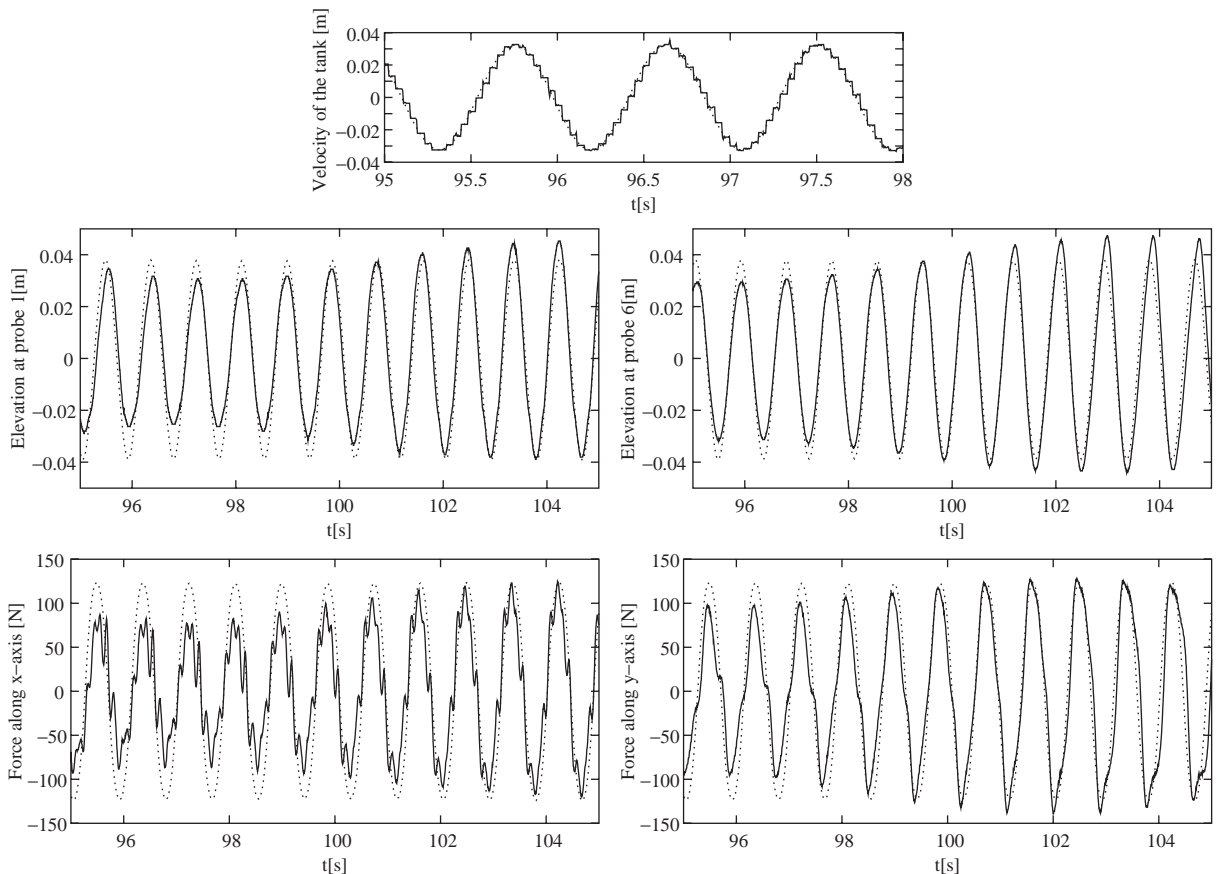


Fig. 6. Comparison of the computed (dotted line) and measured (solid line) velocity of the tank, wave elevations and horizontal force components F_x and F_y for the nearly steady resonant regimes in a square base tank. Computations are made with initial conditions derived from steady state asymptotic solutions by Faltinsen and Timokha (2002a). Diagonal excitation resulting in diagonal waves. $H = 0.0078, h = 0.508, \sigma/\sigma_1 = 1.034$.

steady state regime. Appropriate approximate initial conditions may then be calculated by using asymptotic periodical solutions given by Faltinsen et al. (2003). However, since the last initial conditions are based on asymptotic approximation of the periodical solutions, the simulations by the second scenario cause a beating in the initial phase.

Unfortunately, the first scenario was in many cases not successful, especially for longitudinal forcing. A reason for this is that when the tank is forced along the Ox -axis, the terms in the bracket next to $P_{0,1}^{(2)}$ and $P_{0,3}^{(2)}$ become zero and zero-initial conditions for the modal functions caused always zero transversal waves, i.e. $b_1 = b_2 = b_3 = c_{11} = c_{12} = c_{21} \equiv 0$. The wave motion was then defined by nonzero a_1, a_2 and a_3 and the numerical results were fully consistent with already reported simulations by Faltinsen et al. (2000) for two-dimensional fluid sloshing. Small speculative initial perturbations of the initial conditions did not improve the situation: in the frequency domains of planar waves they led to two-dimensional sloshing after 10–30 forcing periods, while in the region of three-dimensional waves those perturbations resulted in strong amplification of higher modes (it was sometimes so significant that it caused numerical divergence) and the simulations were stopped after 30–40 forcing periods as physically unrealistic ones. In addition, even small speculative changes of the initial perturbation illustrated sometimes qualitatively different wave behaviour. Since nonlongitudinal forcing makes the equation for transversal modes (first of all, Eq. (8b) for the primary dominant mode) inhomogeneous (so that the nonlinear terms cause the modal functions $b_1, b_2, b_3, c_{11}, c_{12}$ and c_{21} to be nonzero), we applied a zero-initial condition scenario for diagonal excitations. Here, however, it led in almost all series to similar results, namely, to either steady state ‘diagonal’ waves (in agreement with steady state analysis) or to amplification of higher modes.

The second scenario demonstrated almost always clear identification of the waves and good agreement with experiments. The simulations were performed for all types of the wave motions. These were especially in good agreement for planar waves (longitudinal excitations) and diagonal waves (diagonal excitation) with frequencies slightly away from the main resonance. About 150–300 forcing periods were needed to get periodic numerical solutions for these resonant wave motions (the criterion for numerically obtained steady state values was that the relative deviation

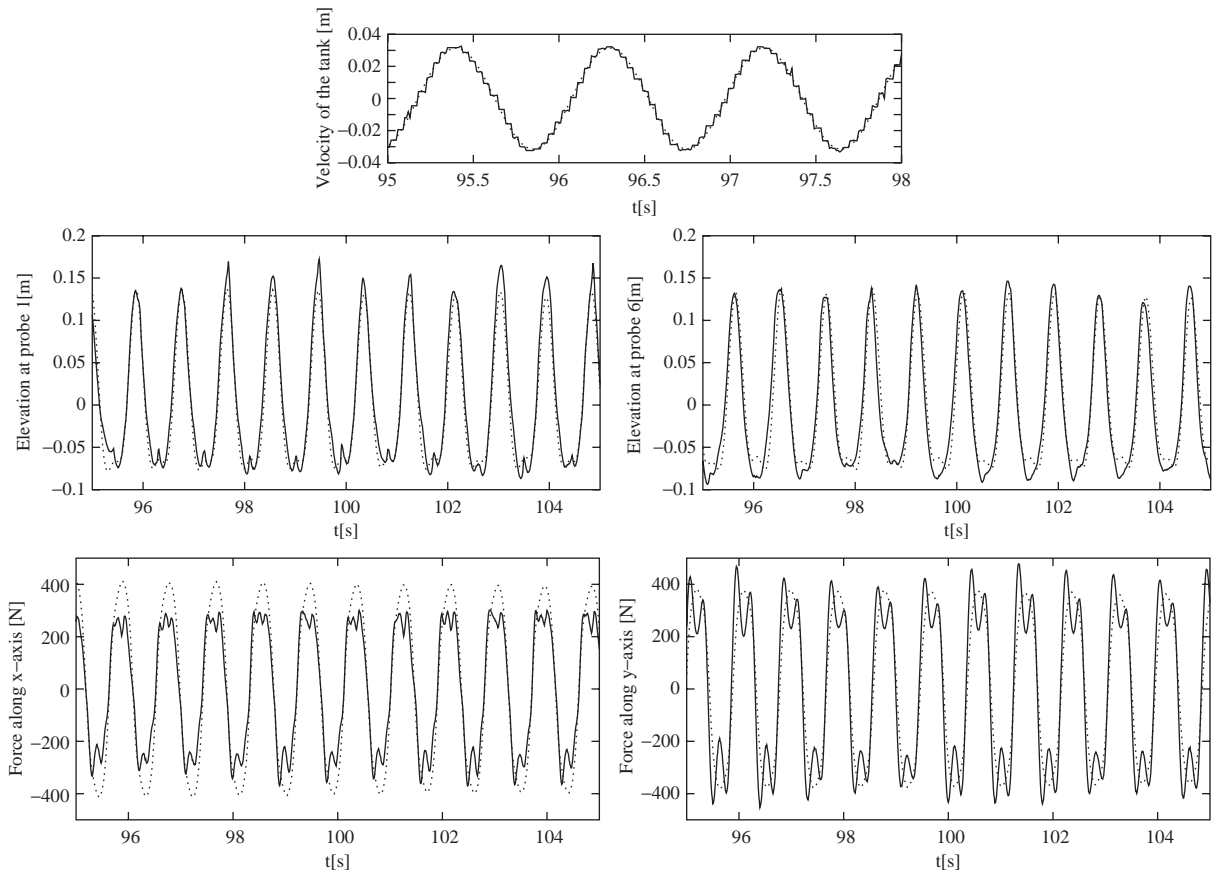


Fig. 7. The same as in Fig. 6, but for diagonal excitation resulting in ‘swirling’ wave. $H = 0.0078, h = 0.508, \sigma/\sigma_1 = 1.0087$.

between maximum beating amplitude and averaged amplitude is 10^{-4}). However, even this scenario showed that three-dimensional resonant waves are very sensitive to small changes in initial conditions. Sometimes the numerical solutions were very close, but clear steady state regimes were not achieved even after 2000 forcing periods. In addition, if an experimental series demonstrated stable three-dimensional steady state waves, but this modal theory did not confirm that, the simulations were unsuccessful leading to numerical divergence due to unrealistic numerical amplifications of higher modes. Since the viscous damping is accounted for, this is an indication that the model may need some modifications in particular by ordering the higher modes in a different way. Effects of local phenomena (local breaking, run-up, near-corner flows, etc.) may also matter.

5.3. Validation by experiments

The theoretical results were experimentally validated by comparing with the measured wave elevation near the wall (probes 1 and 6) and horizontal force components F_x and F_y . The measurements included the inertia force from the tank mass. This relatively small contribution is added to the calculated sloshing force in the presented data. The typical examples for $h = 0.508$ when our previous classification agreed well with experiments are presented in Figs. 6–11 (the measurements are denoted by solid lines, while the numerical simulations are given by dotted lines). The second row in the figures compares the wave elevation, the third row presents measured and calculated hydrodynamic forces. The measured and theoretical forcing velocities of the tank are presented on the top of each figure. The stepwise behaviour is due to a low-frequency output (47 Hz) in the velocity feedback from the closed loop steering system. The real tank motion is smooth.

The first example in Fig. 6 is related to ‘diagonal’ (three-dimensional) waves occurring due to diagonal forcing. Although it demonstrates good agreement between theoretical predictions and measured data for both wave elevation

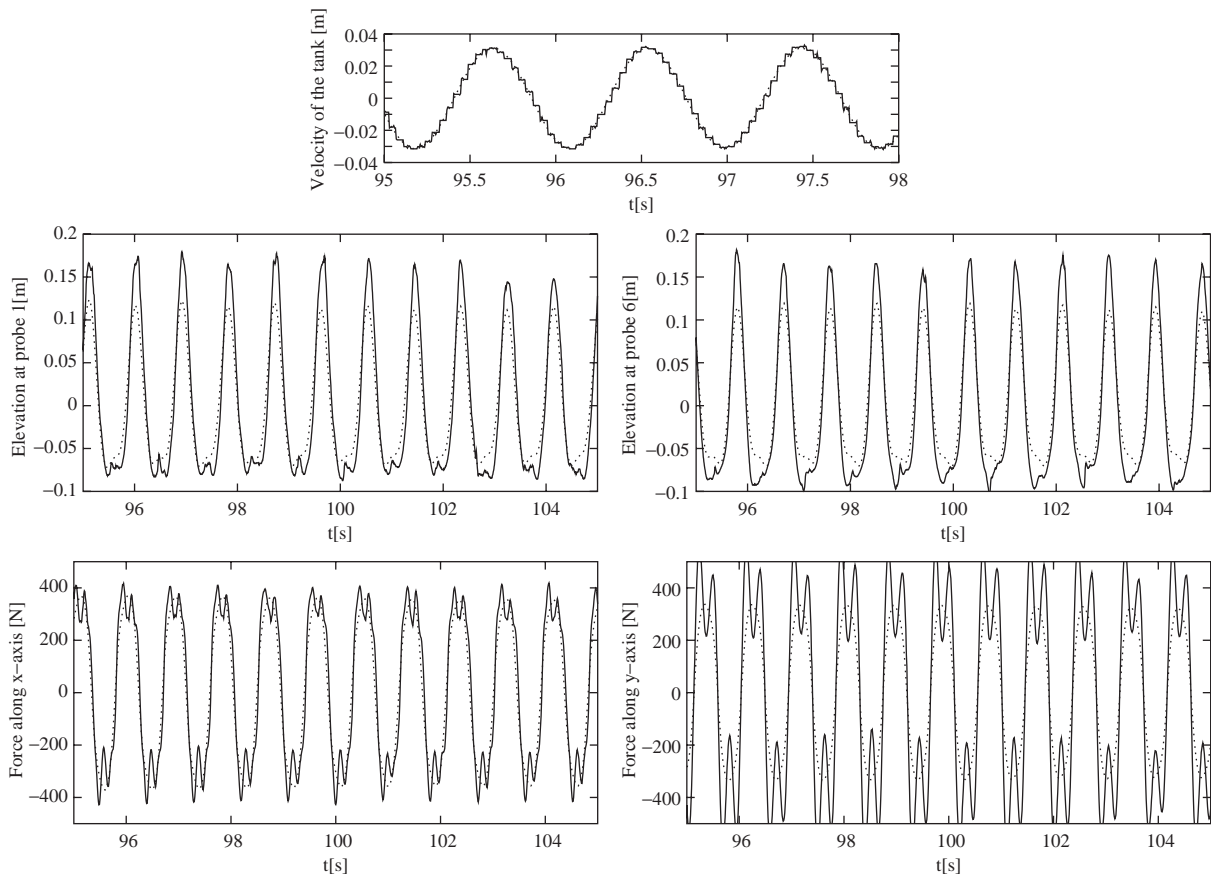


Fig. 8. The same as in Fig. 7, but $\sigma/\sigma_1 = 1.0031$.

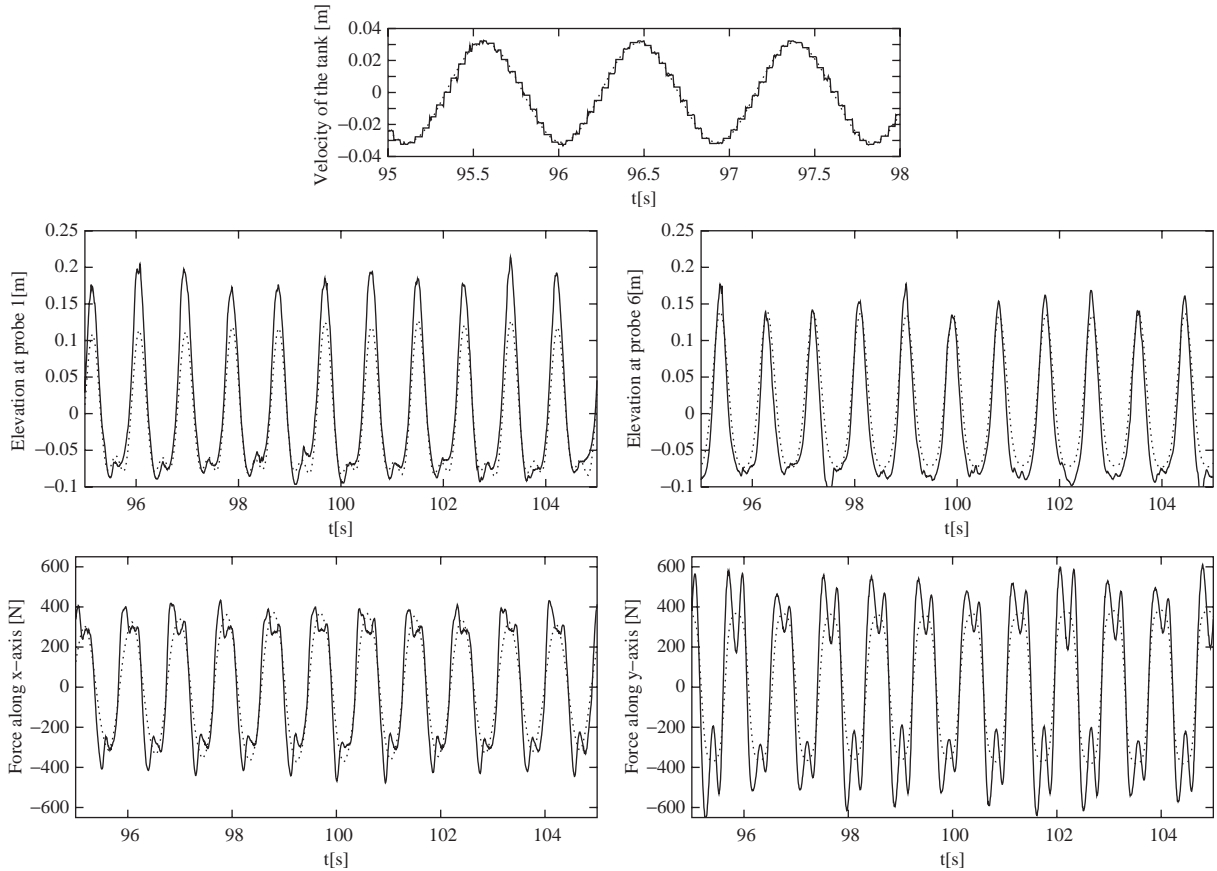


Fig. 9. The same as in Fig. 6, but for longitudinal (surge) excitation resulting in ‘swirling’ wave. $H = 0.0078$, $h = 0.508$, $\sigma/\sigma_1 = 0.9971$.

and the forces, one should note an asymmetry in the experimental data. There is both a difference between the measured wave elevations at 1 and 6, and analogously, a difference in the measured forces F_x and F_y . Due to the symmetry of the system there should be no differences in steady state conditions. The calculations show this symmetry. The asymmetric measured data are likely to be explained by transient phenomena associated with wave perturbations perpendicular to the diagonal forcing plane.

The next examples in Figs. 7 and 8 are for ‘swirling’ waves occurring due to diagonal forcing. These two experimental series were made with only 0.5% difference in the excitation frequency and we originally expected practically equal results. This was true for the theory, but experiments gave up to 20% difference for these two series, especially for the wave elevations. Once more the transient effects are a possible explanation. The importance of the transients and initial conditions are also documented by two cases in Figs. 9 and 10 for longitudinal excitation. In a similar way as in Figs. 7 and 8 the excitation parameters are approximately the same and the theory gives very close results, but the experiments differ from each other, especially for the measured forces.

An important factor affecting the transient character of three-dimensional sloshing is the run-up phenomena established in all the experimental series [see also similar observations by Royon et al. (2002)]. When a ‘swirling’ wave occurs there is particularly strong run-up in terms of thin jets in the tank corners (see photos in Fig. 12). In general, these local phenomena cannot significantly affect the hydrodynamic forces, but may affect the measured wave elevation. This is implicitly confirmed by the case in Fig. 11, where the forces are in good agreement with experiments, while the maximum wave elevations have up to 20% difference.

Figs. 6–11 show clearly higher harmonics $3\sigma - 5\sigma$ in the measured forces F_x and F_y and measured elevations (except, probably elevations in Fig. 6). These are not found in the calculations. These harmonics occur in numerical simulations if either speculative changes of the initial conditions are made or perturbations of higher modes are introduced during the transient phase. This speculative strategy can be defended when the damping is small as it is in our

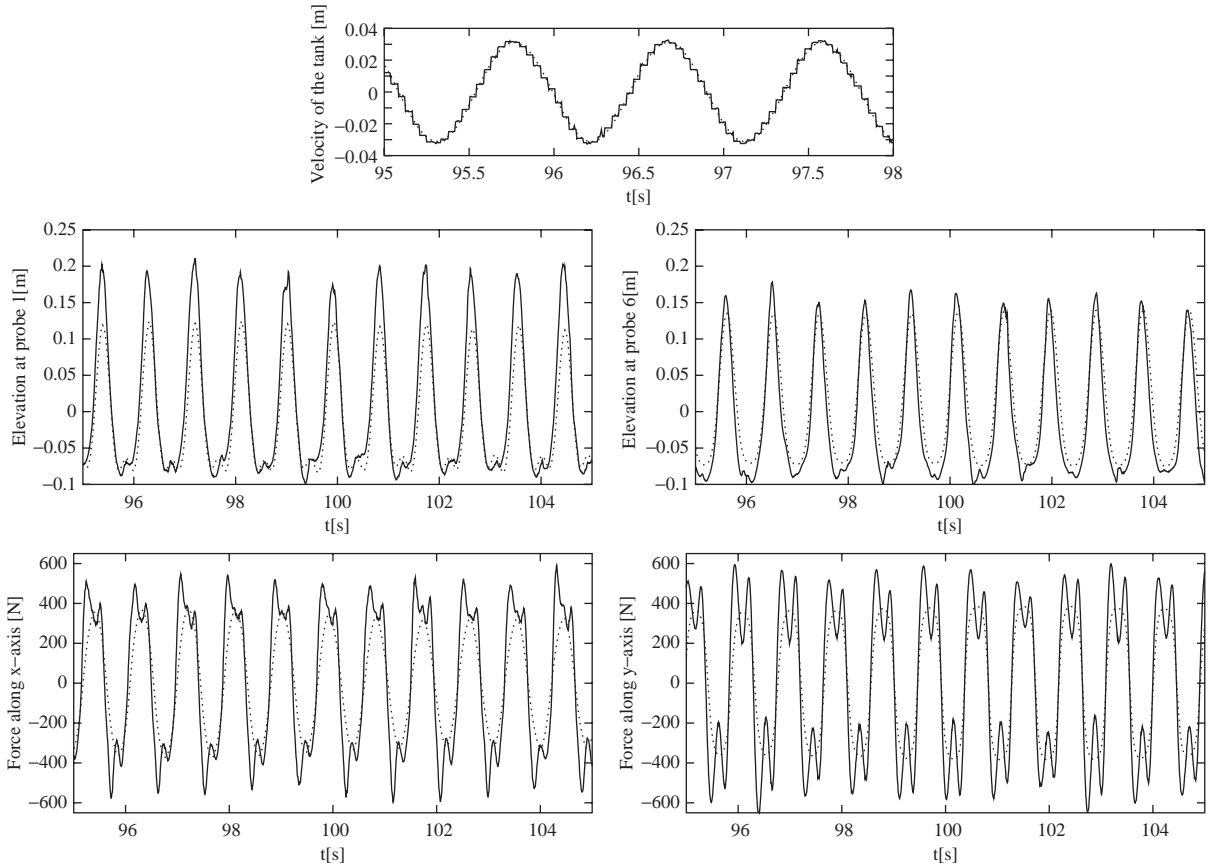


Fig. 10. The same as in Fig. 9, but $\sigma/\sigma_1 = 0.9975$.

case and there are either clearly nonzero initial conditions or local near wall phenomena due to run-up. Why there is a smaller effect of the higher harmonics in wave elevation than in forces follows from our general expressions for wave elevation (1) and the force components (14), (15). The wave elevation depends on the modal functions, while the force depends on the second derivative of the modal functions. According to (15) the dominating modes a_1 and b_1 determine the main contribution to the horizontal forces. Let us say a_1 and b_1 have a 3σ -component expressed as $C \cos(3\sigma t)$. The second derivative of this term is $-(9\sigma^2)C \cos(3\sigma t)$, i.e. the contribution from the 3σ -component is relatively more important for the forces than for wave elevation. A reason why our asymptotic modal theory does not show any pronounced effect of higher harmonics is that our initial conditions are calculated from (16) and the lowest-order terms of a_1 and b_1 in the steady state solution (16) contain only σ -harmonics. Higher-order asymptotic solutions by Faltinsen et al. (2003) showed that the 3σ -component in the dominating modal functions for steady state motions is proportional to $\mathcal{O}(\epsilon)$. This is a too small value to influence our predictions when they are based on periodic initial conditions following from (16). Situations could only change when reordering the modal system by assuming effects of secondary resonance. Then $a_1 \sim a_2$, $b_1 \sim b_2$. Since the modal equations for the primary modes (8a) and (8b) contain the terms $\ddot{a}_1 a_2$, $\ddot{b}_1 b_2$, which are of $\mathcal{O}(\epsilon^{2/3})$, the 3σ -component in dominating modes becomes $\mathcal{O}(\epsilon^{2/3})$. Multiplied by 9 (in calculations of the force components) those terms may in practice become comparable with the primary order term $\mathcal{O}(\epsilon^{1/3})$. Future studies are needed to evaluate the effect of secondary resonance.

6. Conclusions

The use of the information on possible steady state sloshing is a natural way to systematize (classify) the flows due to external resonant forcing. Faltinsen et al. (2003) extracted the asymptotic periodic solutions of the modal system

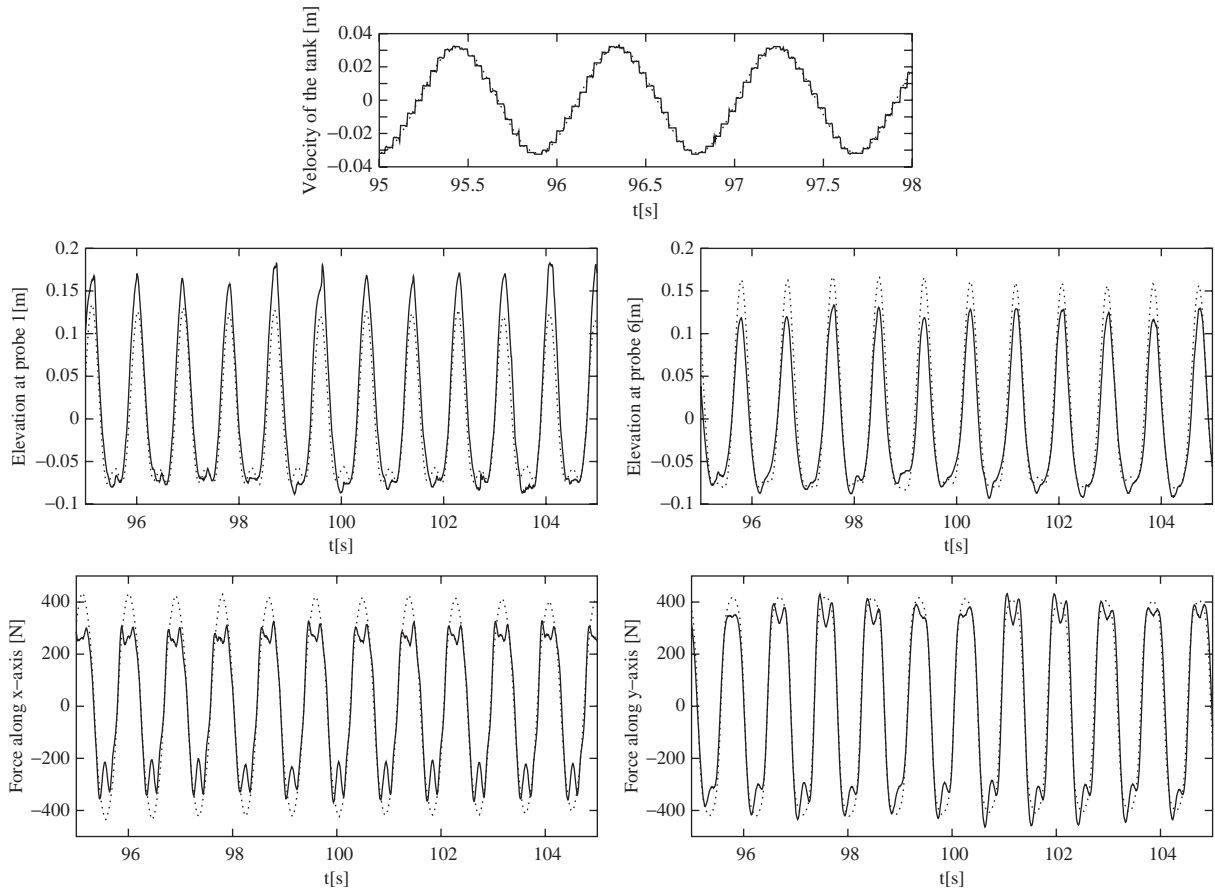


Fig. 11. The same as in Fig. 9, but $\sigma/\sigma_1 = 1.011$.

describing the steady state waves and presented a scheme to study their stability. We used this analytical scheme to classify possible resonant sloshing in a wide range of excitation frequencies/amplitudes for $h > 0.2$ [the last inequality is the limit of the quantitative applicability of the finite water depth theory established by Faltinsen and Timokha (2002a)]. Special emphasis is placed on experimental (both qualitative and quantitative) validation of the modal theory to indicate the effective frequency domain of three-dimensional ‘chaotic’ (no stable steady regime for these input data) and ‘swirling’ (rotary waves) sloshing. It was confirmed that the theoretical predictions of the effective frequency domain are in good agreement for sufficiently large depths (the experimental series with $h = 0.508$), but the theory disagrees slightly for lower depths (especially in the experimental series with longitudinally forced sloshing with $h = 0.27$). The mentioned discrepancy consists in a shift of ‘swirling’ and planar steady state waves into an effective domain of ‘chaotic’ motions. The last motions were not established in the predicted zone for our experimental series with $h = 0.27$. This disappearance was theoretically expected only at $h = 0.23$. Since a two-dimensional analogy of the given modal theory is the system by Faltinsen et al. (2000), which also became inapplicable for $h \leq 0.27$, the discrepancy may be explained in a similar way. Modifications are needed to account for the nonlinearities associated with secondary resonance and dissipation (Faltinsen and Timokha, 2001, 2002a). The experiments confirmed the existence of ‘diagonal’-like steady state waves (three-dimensional free surface fluid motions occurring with small angle to the diagonal plane of the tank) in predicted ranges of the excitation frequencies for $h \leq 0.34$.

Based on the asymptotic modal system the paper gives new classification of steady state regimes for diagonal excitations (horizontal resonant forcing in the diagonal plane of the tank) versus h , excitation frequency and amplitude. In contrast to longitudinal forcing the ‘chaotic’ regimes are only possible in very narrow regions for $h > 0.5$ and around $h = 0.3$. The ‘diagonal’-like (occurring with small angle to the diagonal plane of the tank) waves are not stable except for small effective domains. Therefore the resonant motions are almost always related to ‘diagonal’ waves and ‘swirling’. The most interesting point is that ‘diagonal’ waves are always stable for sufficiently small h . This occurs in

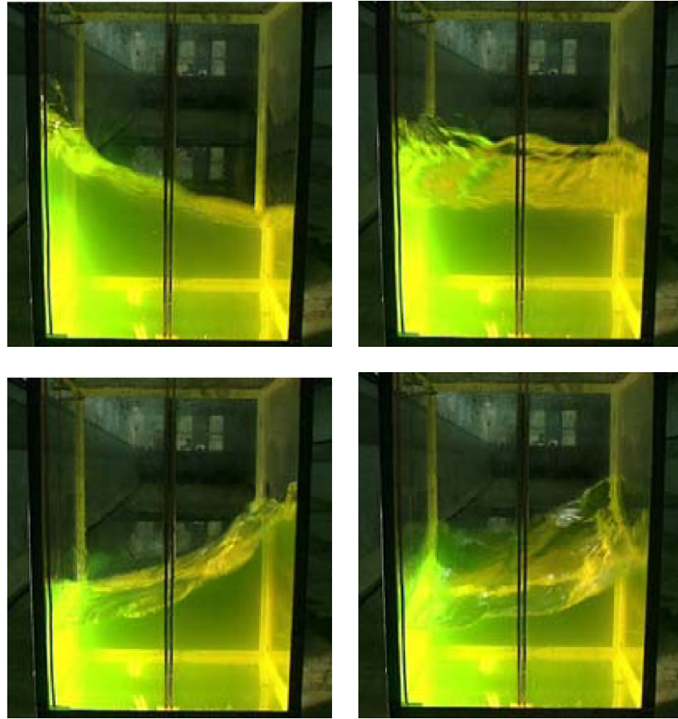


Fig. 12. Photos from the experimental series demonstrating local phenomena near the wall occurring for three-dimensional waves.

our calculations for $h < 0.24 - 0.27$ (depending on the excitation amplitude). An additional point is the presence of a significant frequency domain at $\sigma = \sigma_1 = \sigma_{0,1} = \sigma_{1,0}$, where stable diagonal and ‘swirling’ waves co-exist. If both waves are of approximately equal energy, we could not conclude from the experimental observations and measurements which of the steady state motions would be realized. These cases showed permanent beating and cyclic changes between ‘swirling’ and diagonal wave motions during the experiments. Three-dimensional sloshing with finite depth is characterized by small damping and it is therefore very sensitive with respect to initial perturbations and changes of the frequency/amplitude of the external forcing. The paper discusses these problems in the framework of the extensive comparison of the direct numerical simulations and experimental measurements (wave elevation and horizontal hydrodynamic forces).

The modal theory is validated quantitatively, i.e. the paper considers a series of typical numerical simulations of three-dimensional sloshing. In order to avoid speculations on a possible viscous damping effect, we derived the formulae for linear logarithmic decrements due to viscosity in the fluid bulk and on the tank surface (due to boundary layer formation). These damping terms were incorporated in corresponding modal equations. When using the asymptotic solution by Faltinsen et al. (2003) for calculation of the initial conditions, the numerical series with the damping terms in most cases lead to periodic solutions (relative error 10^{-3} – 10^{-4}) after 150–300 forcing periods. However, they did not give numerical periodic solutions of three-dimensional waves in all the cases. Even if the initial conditions were calculated from the asymptotic approximation of the periodic solution and damping was included, simulations with up to 2000 forcing periods showed beating in simulating the three-dimensional motions. Similar behaviour is typical also in experimental observations, where nonnegligible beating was accompanied by contribution of the higher harmonics (3σ and 5σ), especially in the measured force. Although the experimental and numerical data are generally in good agreement for steady state motions, the simulations typically do not capture those higher harmonics. The problem of higher harmonics in force response is extensively discussed in the main text. They can appear in numerical solutions due to transient effect (speculative change of the initial conditions), local near wall phenomena like run-up, which is especially large at tank corners, or due to effect of secondary resonance by higher modes accompanied by their amplification. The last phenomenon should probably be of primary concern for future studies. Theoretical investigation of the secondary resonance for two-dimensional sloshing with finite depth was

documented by Faltinsen and Timokha (2001). A corresponding theoretical analysis in the three-dimensional case is much more tedious, but seemingly, it should be done.

Finally, we would like to stress again the importance of systematic studies of dissipation in strongly nonlinear sloshing, especially for intermediate depths. Existing estimations of the logarithmic decrements are almost always related to linear sloshing, but the experiments detect a nonlinear nature of the damping caused in many cases by local breaking and run-up. Taking into account the results by Rognebakke and Faltinsen (2000) on damping due to roof impact one finds time-dependent, random, impulsive damping rates of significant value due to local phenomena [some empirical/phenomenological theories based on a pendulum model of the sloshing to account for fluid wall impact are reviewed by Ibrahim et al. (2001)]. However, we have still no theoretical strategy on how to perform corresponding modifications in the multidimensional modal systems. Another interesting direction is to study the wave phenomena in a near-square tank (r is close, but not equal to 1). Bridges (1985, 1987) established some new types of free nonlinear sloshing with even infinitesimal deviation of r from 1. Although the modal methods should capture these nonlinear wave motions, the paper does not give an answer on how a non-square cross-section affects steady state resonant waves.

Acknowledgements

The third author gratefully acknowledges the support of the Alexander-von-Humboldt Foundation (Germany) and Centre of Excellence for Ship and Ocean Structures at NTNU (Norway) in funding the work described here.

References

- Abramson, H.N., 1966. The dynamics of liquids in moving containers. NASA Report, SP 106.
- Abramson, H.N., Bass, R.L., Faltinsen, O.M., Olsen, H.A., 1974. Liquid slosh in LNG Carriers. In: Tenth Symposium on Naval Hydrodynamics. June 24–28, 1974. Cambridge, MA. ACR-204, pp. 371–388.
- Arai, M., Cheng, L.Y., Inoue, Y., 1992. 3D numerical simulation of impact load due to liquid cargo sloshing. *Journal of the Society of Naval Architects of Japan* 171, 177–185.
- Arai, M., Cheng, L.Y., Inoue, Y., 1993. Numerical simulation of sloshing and swirling in cubic and cylindrical tank. *Journal of Kansai Society of Naval Architects, Japan* 219, 97–101.
- Aubin, J.-P., 1972. Approximation of Elliptic Boundary-Value Problems. Wiley-Interscience, New York-London-Sidney-Toronto.
- Barber, N.F., 1969. *Water Waves*. Wykeham Publications, London.
- Bridges, T.J., 1985. On secondary bifurcation of three dimensional standing waves. Technical Summary Report Wisconsin University, Madison.
- Bridges, T.J., 1987. Secondary bifurcation and change of type for three dimensional standing waves in finite depth. *Journal of Fluid Mechanics* 179, 137–153.
- Bryant, P.J., 1989. Nonlinear progressive waves in a circular basin. *Journal of Fluid Mechanics* 205, 453–467.
- Cariou, A., Casella, G., 1999. Liquid sloshing in ship tanks: a comparative study of numerical simulation. *Marine Structure* 12, 183–198.
- Celebi, S.M., Akyildiz, H., 2002. Nonlinear modelling of liquid sloshing in a moving rectangular tank. *Ocean Engineering* 29, 1527–1553.
- Chern, M.J., Borthwick, A.G.L., Eatock Taylor, R., 1999. A pseudospectral σ -transformation model of 2-d nonlinear waves. *Journal of Fluids and Structures* 13, 607–630.
- Dean, R.G., Dalrymple, R.A., 1992. *Water Wave Mechanics for Engineers and Scientists*. World Scientific, Singapore.
- Faltinsen, O.M., 1974. A nonlinear theory of sloshing in rectangular tanks. *Journal of Ship Research* 18, 224–241.
- Faltinsen, O.M., Timokha, A.N., 2001. Adaptive multimodal approach to nonlinear sloshing in a rectangular tank. *Journal of Fluid Mechanics* 432, 167–200.
- Faltinsen, O.M., Timokha, A.N., 2002a. Asymptotic modal approximation of nonlinear resonant sloshing in a rectangular tank with small fluid depth. *Journal of Fluid Mechanics* 470, 319–357.
- Faltinsen, O.M., Timokha, A.N., 2002b. Analytically-oriented approaches to two-dimensional fluid sloshing in a rectangular tank (survey). *Proceedings of the Institute of Mathematics of the Ukrainian National Academy of Sciences Problems of Analytical Mechanics and its Applications* 44, 321–345.
- Faltinsen, O.M., Rognebakke, O.F., Lukovsky, I.A., Timokha, A.N., 2000. Multidimensional modal analysis of nonlinear sloshing in a rectangular tank with finite water depth. *Journal of Fluid Mechanics* 407, 201–234.
- Faltinsen, O.M., Rognebakke, O.F., Timokha, A.N., 2003. Resonant three-dimensional nonlinear sloshing in a square base basin. *Journal of Fluid Mechanics* 487, 1–42.
- Ferrant, P., Le Touze, D., 2001. Simulation of sloshing waves in a 3D tank based on a pseudo-spectral method. In: *Proceedings of 16th International Workshop on Water Waves and Floating Bodies*, Hiroshima, Japan.

- Fultz, D., 1962. An experimental note on finite-amplitude standing gravity waves. *Journal of Fluid Mechanics* 13, 193–212.
- Gavrilyuk, I., Lukovsky, I.A., Timokha, A.N., 2000. A multimodal approach to nonlinear sloshing in a circular cylindrical tank. *Hybrid Methods in Engineering* 2 (4), 463–483.
- Gerrits, J., 2001. Dynamics of liquid-filled spacecraft. Numerical simulation of coupled solid–liquid dynamics. Ph.D. Thesis, Rijksuniversiteit Groningen.
- Hill, D.F., 2003. Transient and steady-state amplitudes of forced waves in rectangular. *Physics of Fluids* 15 (6), 1576–1587.
- Ibrahim, R.A., Pilipchuk, V.N., Ikeda, T., 2001. Recent advances in liquid sloshing dynamics. *Applied Mechanics Research* 54 (2), 133–199.
- Keulegan, G.H., 1959. Energy dissipation in standing waves in rectangular basin. *Journal of Fluid Mechanics* 6, 33–50.
- La Rocca, M., Mele, P., Armenio, V., 1997. Variational approach to the problem of sloshing in a moving container. *Journal of Theoretical and Applied Fluid Mechanics* 1 (4), 280–310.
- La Rocca, M., Sciortino, G., Boniforti, M.A., 2000. A fully nonlinear model for sloshing in a rotating container. *Fluid Dynamics Research* 27, 23–52.
- Landau, L.D., Lifshitz, E.M., 1987. *Course of theoretical physics. Fluid Mechanics*. 2nd ed., vol. 6. Pergamon Press, Oxford.
- Lukovsky, I.A., 1990. Introduction to the nonlinear dynamics of a limited liquid volume. *Naukova Dumka, Kiev* (in Russian).
- Lukovsky, I.A., Timokha, A.N., 2002. Modal modeling of nonlinear sloshing in tanks with non-vertical walls. Non-conformal mapping technique. *International Journal of Fluid Mechanics Research* 29 (2), 216–242.
- Lukovsky, I.A., Barnyak, M.Ya., Komarenko, A.N., 1984. Approximate methods of solving the problems of the dynamics of a limited liquid volume. *Naukova dumka, Kiev* (in Russian).
- Mikishev, G.I., 1978. Experimental methods in the dynamics of spacecraft. *Mashinostroenie, Moscow* (in Russian).
- Miles, J.W., 1994. Faraday waves: rolls versus squares. *Journal of Fluid Mechanics* 269, 353–371.
- Moore, R.E., Perko, L.M., 1964. Inviscid fluid flow in an accelerating cylindrical container. *Journal of Fluid Mechanics* 22 (2), 305–320.
- Moiseyev, N.N., 1958. To the theory of nonlinear oscillations of a limited liquid volume of a liquid. *Journal of Applied Mathematics and Mechanics (PMM)* 22, 612–621 (in Russian).
- Moiseyev, N.N., Romyantsev, V.V., 1968. *Dynamic Stability of Bodies Containing Fluid*. Springer, New York.
- Narimanov, G.S., 1957. Movement of a tank partly filled by a fluid: the taking into account of non-smallness of amplitude. *Journal of Applied Mathematics and Mechanics (PMM)* 21, 513–524 (in Russian).
- Narimanov, G.S., Dokuchaev, L.V., Lukovsky, I.A., 1977. Nonlinear dynamics of flying apparatus with liquid. *Mashinostroenie, Moscow* (in Russian).
- Ockendon, J.R., Ockendon, H., 1973. Resonant surface waves. *Journal of Fluid Mechanics* 59, 397–413.
- Ockendon, H., Ockendon, J.R., Waterhouse, D.D., 1996. Multi-mode resonance in fluids. *Journal of Fluid Mechanics* 315, 317–344.
- Perko, L.M., 1969. Large-amplitude motions of liquid–vapour interface in an accelerating container. *Journal of Fluid Mechanics* 35 (1), 77–96.
- Perlin, M., Schultz, W.W., 2000. Capillary effects on surface waves. *Annual Review of Fluid Mechanics* 32, 241–274.
- Rognebakke, O.F., Faltinsen, O.M., 2000. Damping of sloshing due to roof impact. In: *Proceedings of 15th International Workshop on Water Waves and Floating Bodies*. 27. February–1. March 2000. Dan Caesarea Hotel, Israel.
- Royon, A., Gaudin, E., Cavellier, A., Hopfinger, E.J., 2002. Sloshing and drop formation conditions in cylindrical liquid propellant tanks. In: *Abstracts of fourth International Conference on Launcher technology, “Space Launcher Liquid Propulsion”*, Liege, Belgium, 3–6 December, 2002.
- Shankar, P.N., Kidambi, R., 2002. A modal method for finite amplitude, nonlinear sloshing. *Pramana—Journal of Physics* 59 (4), 631–651.
- Timokha, A.N., 2002. Note on ad hoc computing based upon a modal basis. *Proceedings of the Institute of Mathematics of the Ukrainian National Academy of Sciences: Problems of Mechanics and its Applications* 44, 269–274.
- Tomawa, S., Sueoka, H., 1989. Experimental and numerical studies on sloshing in partially filled tank. *The Proceedings of the Fourth International Symposium on Practical Design of Ships and Mobile Units*, vol. 57, pp. 1–57.8.
- Waterhouse, D.D., 1994. Resonant sloshing near a critical depth. *Journal of Fluid Mechanics* 281, 313–318.
- Yalla, S., 2001. Liquid dampers for mitigation of structural response: theoretical development and experimental validation. Ph.D. Thesis, Department of Civil Engineering and Geological Sciences, Notre Dame, Indiana.
- Zakharov, V.E., 1968. Stability of periodic waves of finite amplitude on the surface of a deep fluid. *Journal of Applied Mechanics and Technical Physics* 2, 190–194.